Ground Penetrating Radar as a Subsurface Environmental Sensing Tool

LEON PETERS JR., LIFE FELLOW, IEEE, JEFFREY J. DANIELS, AND JONATHAN D. YOUNG, MEMBER, IEEE

Invited Paper

Ground Penetrating Radar (GPR) is considered as an environmental tool. The basic concepts involved in GPR are introduced briefly including the antennas, propagation, target scattering, and mapping. Target identification is important when using GPR since the scatterer can only be observed by evacuation. This is discussed in terms of mapping and Complex Natural Resonances. GPR has been used and is being considered as a tool for the detection of a wide variety of subterranean features. A very brief description of the various applications of GPR is presented. In terms of environmental sensing, it has been applied to detect buried tanks, landfill debris, water levels, and contaminated fluids. The detection of various military devices also represent a serious environmental concern including land mines and unexploded ordnance. There are also possible applications involving the detection of buried utilities highway voids, grave sites. It has been used for examining archeological sites. The above list is far from complete because of the ever-expanding use of GPR.

I. INTRODUCTION

Ground Penetrating Radar (GPR) can be defined as a radar whose goal is to detect and identify structures within the ground. The properties of such a radar are restricted to the frequency, bandwidth, etc., that are required to detect the desired target, either natural or man-made, in the presence of a lossy, possibly inhomogeneous medium. Propagation losses, antenna size, and size of the scatterer to be detected dictate the frequency band of operation.

For example, in clay losses can be 100 dB/ft or more at X-band frequencies but only a few decibels per foot at HF/VHF/UHF frequencies [1]. The lower frequency may be fixed by mobility constraints since an antenna that is too large has only limited usefulness, particularly if a very large surface is to be scanned by the GPR. Scatterer size also represents a factor. A land mine, for example, is a very small scatterer and requires frequencies from 100 to 500 MHz be used. A large unexploded shell immersed in clay may be resonant for frequencies as low as 10 MHz. A planar geological interface would be represented as the image of the antenna in that interface and scatterer size is not a factor. Two GPR review papers have been published previously [2], [3].

Ground Penetrating Radar (GPR) can be considered at best to be an imperfect technology. However, at three different government sponsored workshops to evaluate techniques for detecting subsurface targets [4]–[6], the general consensus was that for reasonably shallow targets, GPR was the major hope for detecting and identifying subsurface anomalies.

While much of the research involving GPR has been directed toward military operations, it is the conversion to nonmilitary applications such as environmental concerns that is important in today's requirements. Even previous military studies such as the detection of mines and unexploded ordnance fit this category. For example, mines saturate many areas where combat has occurred such as Afghanistan, the Falkland Islands, Vietnam, and Saudi Arabia. Even in the United States, unexploded ordnances (UXO's) also represent a serious problem in making test ranges safe. These items must be detected and neutralized before these vast areas can be converted to nonmilitary use. Another military topic, tunnel detection, also has a counterpart in the environmental community which is subsidence detection. In Columbus alone there have been two major highway collapses, one at the very center of the city and another that closed a major section of I-70. Other examples are abandoned shallow mines particularly in northern Ohio and elsewhere. There are also a number of applications more obviously related to environmental issues such as detecting chemical spills, nuclear waste, grave sites, various underground utilities, etc.

Ground Penetrating Radar concepts have been in use for about 20 years in contrast to more than 50 years for conventional radar systems. The original incentive for its

Manuscript received May 6, 1994.

L. Peters, Jr. and J. D. Young are with the ElectroScience Laboratory, Department of Electrical Engineering, The Ohio State University, Columbus, OH 43212 USA.

J. D. Daniels is with the Department of Geological Sciences, The Ohio State University, Columbus, OH 43210 USA.

IEEE Log Number 9405552.

0018–9219/94$04.00 © 1994 IEEE

development was military in nature. Lerner obtained a patent in 1974 [7]. The application was the detection of tunnels and buried mines. Neither has been a sparkling success. Tunnels in Korea were detected only through intelligence information. Land mines were easily detected [8]–[10], but mobility and identification represented problems, particularly in view of the large variety of shapes of such mines and of false targets. Patents were also issued to Morey in 1974 [11] and to Young and Caldecott in 1976 and 1977 [12], [13].

Utilities (pipes, power lines, etc.) represent another possible application. The ElectroScience Laboratory (ESL) under gas company sponsorship developed a radar subsequently produced by MACOM known as the Terrascan [14]. The goal was the detection of 90% of plastic pipe in 90% of the country. A series of tests revealed that approximately an 80/80% was achieved. This was never adopted by the gas industry, even though there was no other viable method of plastic pipe detection because of potential liabilities.

In spite of these limited successes GPR has become of intense interest to geophysicists. There were 45 papers presented at GPR symposium in Finland in 1992 [15] and 67 papers were presented at a similar conference in a GPR symposium in Colorado in 1990 [16]. It is of interest to note that most of these papers were directly related to environmental concerns and a variety of applications were covered including geological structures and even buried corpses. At a GPR workshop co-sponsored by the Environmental Protection Agency (EPA) just completed at OSU, there were 163 attendees [17] from government, industry, and universities. It would require a devoted paper simply to summarize the various nonmilitary applications discussed in these references alone. There have indeed been a large number of such GPR applications in the past but there will be even greater needs in the future. Many of these applications are described in various symposia and workshops.

Because of the deceptively simple GPR structure, there are a number of such GPR units that have been designed and built on an individual need basis by the user. Clearly the bulk of activity in GPR is experimental and has been focussed on the particular target of interest for that user. Much of this activity is focussed on the detection and mapping of interfaces in the earth. From an environmental viewpoint, the tracking of oil spills or other sources of pollution is of interest and will be discussed in more detail later.

There are today commercial versions of GPR available from various manufacturers. Geophysical Survey Systems Inc., Sensors and Systems, Vadose, and Century Geophysical exhibited and tested systems at the recent EPA funded workshop [17] under rather stringent conditions at the ElectroScience Laboratory. There are other manufacturers of such GPR.

There are several major difficulties in GPR design and usage that are not inherent in more conventional radar design. Since the usual GPR has a much broader bandwidth than even the so-called Ultra Wide Band Radars [18] that have been investigated in recent years, they are extremely vulnerable to interference. This can be reduced by averaging a number of returns obtained as a function of time without moving the antenna. However, signals generated by various types of clutter are not reduced by signal averaging. Clutter can be subdivided into various categories including multiple internal reflections, scattering generated by surface roughness, and scattering from undesired buried targets within the radar field of view. Internal reflections are minimized by system design. The other forms of clutter remain as a serious problem. These problems are compounded by poor antenna design. As an example, a pipe distribution system was installed at the ESL approximately 20 years ago by trenching. The soil (clay) was carefully compacted to restore it as closely as possible to its original condition. Data collected immediately after installation clearly showed the presence of the pipe [1], but the subsequent migration of water was disturbed by the trenching process. Today, these pipes are difficult to detect because they are masked by scattering from the trench walls. Obviously, the problem of clutter cannot be eliminated by system design. Its effect can be reduced by antenna design. Most GPR antennas experience ringing as a result of radiating a broad band signal, and this ringing tends to obscure later time signals recorded from any buried scatterer. Reducing the ringing duration then would reduce the clutter in the recorded signal.

From the above discussion, it should be apparent that target identification represents an important step, particularly since one must "dig up" the target to see it. The most usual identification format is that of mapping. There are several possible forms of presentation, some of which are stacking of waveforms obtained as the radar is moved, and observing the change in bright spot position. Other techniques that have been used include the concept of Complex Natural Resonances. These have proven successful for identification of land mines [7]–[9] as mentioned earlier. Various forms of signal processing are of substantial use in GPR interpretation.

II. Ground Penetrating Radar (GPR) Concepts

Since GPR's are quite different from conventional radars, a brief description of some generic models are given in this section. It will encompass various features of GPR's built, used, and suggested at the ESL. No attempt is made to discuss any commercially available units since they probably all involve trade secrets not known to these authors. Most GPR's are basically Time-Domain Reflectometers. They differ in that the signal is radiated into the ground. A simple block diagram is given in Fig. 1. The transient source may be any transient signal. Half a sine wave, steps, and doublets all are possible sources. Our current preference for a source are readily available solid-state pulsers and gas-discharge pulsers to be used when higher power is desired. Pulsewidth and rise time are usually of the order of a few nanoseconds and the repetition rate may range from 1 to 100 kHz. The analysis at the ESL

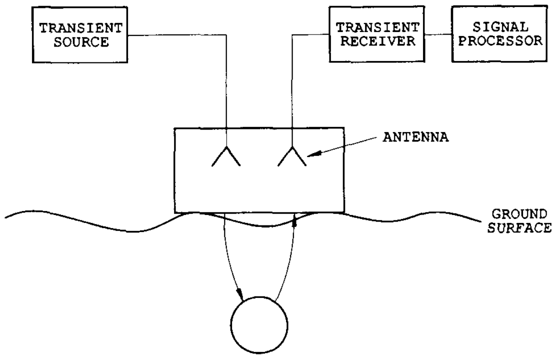

Fig. 1. Block diagram of subsurface-probing radar.

has used a normalized Gaussian pulse shown in Fig. 2 in mathematical models of these sources [19]. The spectrum of such a pulse is extremely broad as compared to even the so-called Ultra Wide Band systems. The use of transients in a radar require that careful matching be achieved at every possible junction and this is usually achieved by matching characteristic or surge impedances and resistive loading. Any use of energy storage devices can lead to excessive multiple reflections that can obscure the desired target. To minimize such problems, the pulser is usually placed as close as is practical to the transmitting antenna so that such multiple reflections are quickly damped. The antenna becomes one source of filtering since an antenna cannot radiate dc. For typical GPR usage, the radiated spectrum may range from a few megahertz to a few gigahertz. The receiver can take the forms of a sampling system or a transient digitizer. The sampling system simply constructs the received waveform from displaced samples of successive periods of the waveform. This sampling system makes it possible to use an amplifier with time- (or range-) dependent gain controlled by a computer prior to the sampler in order to minimize sampling noise. The transient digitizer, on the other hand, is a single-shot device and captures the complete waveform in one period and the time- (or range-) dependent amplifier is no longer applicable because of the response time of the amplifier would be much greater than the width of the nanosecond pulser [20].

Most practical GPR's operate with a fairly consistent set of operating parameters. Pulsewidths range in general from 1 to about 10 ns. Peak transmitter voltage levels operating into 50-Ω cables range from 30 V to several thousand volts. Repetition rates range from about 60 Hz to 1 MHz. Sampling rates, however, are 200 kHz or less. The lower repetition ratios tend to be associated with the higher transmitter voltages and are associated with gas-discharge devices. The higher repetition rates are associated with the lower voltage pulsers and are associated with solid-state pulsers which are more stable. This fixes the spatial resolution before introducing antenna ringing to roughly $1/\sqrt{\epsilon_2}$ to $10/\sqrt{\epsilon_2}$ feet. The average power levels tend to be approximately the same for either case. Sampling systems with no heroic measures such as low-temperature samplers

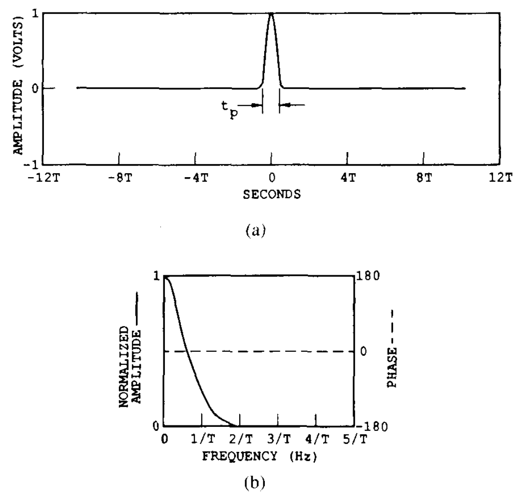

Fig. 2. Normalized Gaussian pulse and its spectrum. (a) Input pulse $t_p = T$ seconds. (b) Input pulse spectrum normalized to $7.344T$ V/Hz.

have a sensitivity of the order of 1 mV. Thus the practical system dynamic range is approximately of the order of 100 dB.

The sampling system has an advantage over the transient digitizer in terms of dynamic range in that there are commercially available samplers with 14-bit A/D converters in contrast to 8-bit A/D's for the transient digitizer. On the other hand, the transient digitizer takes the complete waveform essentially as a snap shot whereas the sampler requires one sample only out of each such waveform. Thus the measurement time to generate and record a complete waveform is much greater for the sampler.

The most critical part of the GPR system is the antenna. These usually take the form of heavily loaded dipoles. The dipoles are heavily loaded to reduce as much as possible the antenna ringing which could extend into the range window of the desired signal. Various combinations of transmit and receive dipoles are used. The most common version is a simple pair of parallel antennas, one for transmit and one for receive as shown in Fig. 3 and is usually designated as a bistatic antenna. This system is used to reduce the direct coupling from the transmitter to the receiver. Other means of reducing this coupling consist of a crossed dipole where the transmit and receive antenna are orthogonal to each other. A more recent antenna has been designated as the time-domain monopulse antenna [21] also shown in Figs. 3 and 4. Identical pulses of opposite polarity are used to excite the two external dipoles. The receiving antenna is placed midway between the two transmitting antennas which reduces the direct coupled signal. It is extremely important that good baluns are used to connect the coaxial cable from the pulser to the antenna. Any unbalance will result in currents flowing on the outside of the cable which in turn can couple strongly to the receiver. This difficulty may be eliminated if the pulser is placed directly at the terminals of the transmitting antenna. Interference is a

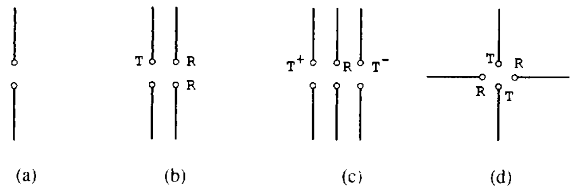

Fig. 3. Generic forms of some GPR antennas. (a) Monostatic antenna—Requires some type of TR device to isolate received signal. (b) Bistatic antenna—Uses separate antennas to isolate received signal. (c) Time-domain monopulse—Includes cancellation scheme to isolate received signal. (d) Crossed dipoles—Uses orthogonal antenna to isolate received signal.

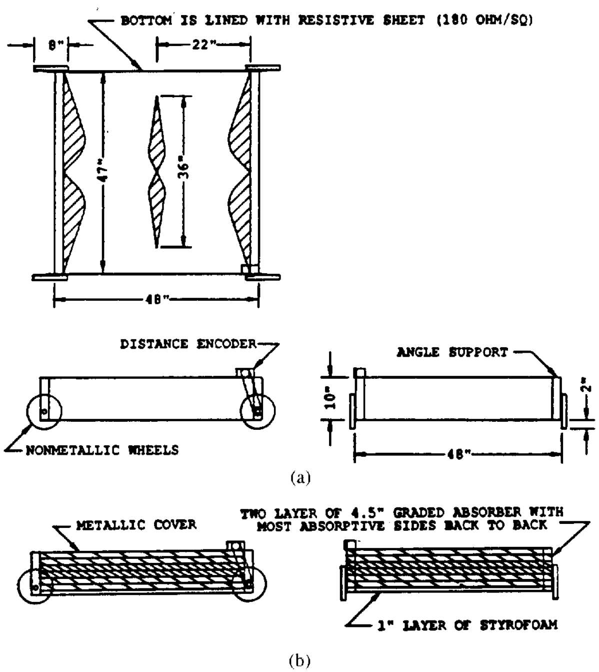

Fig. 4. Structure of the time-domain monopulse. (a) Unshielded. (b) Shielded.

serious problem because these GPR systems must operate over a very broad frequency band. Consequently, this can be alleviated by use of absorbers and conducting shields placed above the absorber. The use of such shields does reduce the effectiveness of the radar in that the clutter caused by the antenna itself is increased [21]. Figure 5 shows a set of measurements for different antennas obtained by inserting the same small target at the same depth in a pipe slanted into the earth. These are merely examples and different antenna construction might lead to slightly different results, see Fig. 5(e) and (f), for example. Obviously, Fig. 5(b) must clearly see the target. The presence of the shield does lead to some degradation of the received signal as seen by comparing Fig. 5(b), (e), and (f).

For these systems, the antenna is spaced only a small distance, 2″ to 3″ above the ground. In some commercial versions, they are mounted in a very rugged cart. As the height above the ground is increased so also is the Radio Frequency Interference.

Even though the dipoles used in these various antennas are heavily loaded, they still represent a bandpass filter. The center frequency of this "bandpass" filter approximately coincides with the frequency where the dipoles are $\lambda/2$ long in their environment including loading by the ground. A typical spectrum of a radiated signal into the earth by one such antenna is shown in Fig. 6 [20]. If the center frequency is to be doubled, then as a first approximation the antenna dimensions would be halved. These patterns were measured using a broadband probe inside the same slant pipe as the measurements of Fig. 5 as the antenna is moved above the pipe in 2.3″ intervals [21]. Several possible antennas exist to extend the operating bandwidth but they do have restrictions. Broadband antennas such as the spiral can be used but they are dispersive. This dispersion must be removed via data processing [22]. More recently, Lai *et al.* [23] have developed antennas with a microslot/microstrip balun that has an extremely wide bandwidth but, in the frequency band required, it is a very large structure. A balun-fed reflector antenna using the supporting struts as feed lines can be defocussed to place a second focussed spot at or below the ground [24]. This is also an extremely large structure but it would have a frequency band restricted only by the reflector size and construction accuracy.

In many of the original studies of GPR there was a comparison of time- and frequency-domain systems such as chirp radar. In the 1970's, the technology was not adequate for a useful frequency-domain system. However, with the advent of Network Analyzers and other similar radar systems such as the radars used in the ESL anechoic chamber [25], it is now possible to build such a radar with adequate speed [19] to act as a GPR. Such a radar can be scanned from 10 MHz to 1 GHz in 10-MHz steps in a small fraction of a second. Such a receiver would have an increased sensitivity and an inherent filtering capability in that the data over the band of an interfering signal would be deleted and filled in by interpolation.

Such a radar system can be made to have an inherent advantage in comparison to the network analyzers by using a tracking filter instead of a harmonic mixer and thus avoid potential problems from intermodulation products. While these stepped frequencies have not yet been used to the best of our knowledge for GPR applications, they have been applied in this frequency band for several Ultra Wide Band Radar applications. Finally, it is noted that the system with a tracking filter has a very narrow bandwidth in comparison to the time-domain system and consequently the inherent noise level is much lower.

III. Propagation and Scattering Attenuation Functions for GPR

The radar range equation is the vehicle for estimating radar parameters when operating in free space. This is not useful for GPR for several reasons. First, operational conditions often dictate that neither the antenna nor the scatterer satisfy far-field conditions implicit in the radar range equation. Second, most GPR antennas are operated

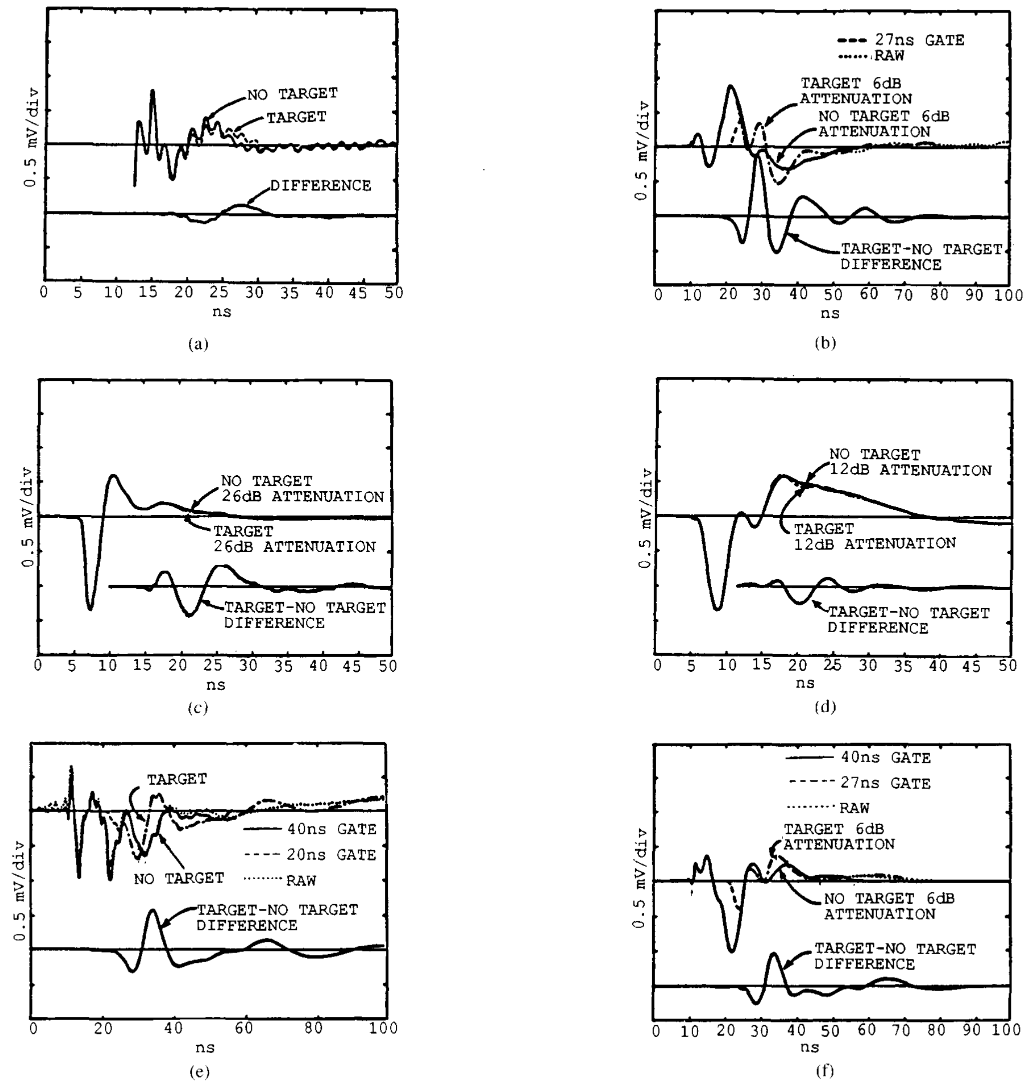

Fig. 5. Time-domain scattering measurements for (a) crossed dipole, (b) original time-domain antenna, (c) parallel loaded dipoles, (d) shielded parallel loaded dipoles, (e) shielded symmetric active isolation antenna, and (f) reconstructed shielded symmetric active isolation antenna.

in the immediate vicinity of the ground interface. This must also be accounted for in the analysis. Third, the medium is highly lossy. Most media are representable as a lossy dielectric where the phase factor is approximated by

$$\beta = \omega\sqrt{\mu\epsilon} \tag{1}$$

and the attenuation factor by

$$\alpha = \frac{1}{2}\sigma\sqrt{\frac{\mu}{\epsilon}} \tag{2}$$

where μ is the permeability, ϵ is the permittivity, and σ is the conductivity of the medium. It is noted that for most soils, the conductivity is frequency-dependent and thus the attenuation factor is **not** independent of frequency as might be assumed from (2).

The model shown in Fig. 7 has been suggested as a means of estimating system performance [25]. This model allows different parameters to become separable. Otherwise, it becomes necessary to do the complete analysis every time any parameter is changed. The model is shown for the case of a cylinder and cross dipole but is applicable to other antenna and scatterer geometries. The quantity E^S/E^I has been designated as the Scattering Attenuation Function (SAF $= E^S/E^I$). The SAF is defined as the modification of the scattered fields by the specified scatterer of a perfect planar reflector. The SAF is derived in [26] for several configurations. These results are summarized in Table 1 as obtained by geometrical optics.

Figure 8 shows the exact computation for the SAF of a circular tunnel [27]. Note that this result is range-

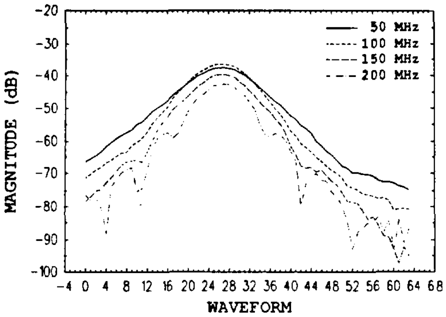

Probe 18" deep in soil, 2.3" between waveforms
($\epsilon_r = 18.9, \sigma = 40.1$ mmho/m)

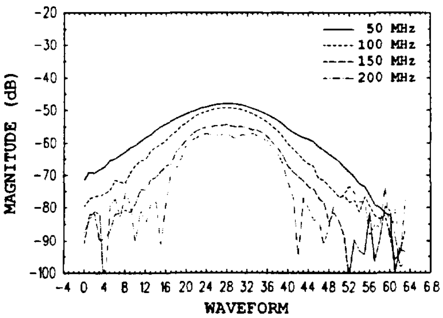

Probe 30" deep in soil, 2.3" between waveforms
($\epsilon_r = 23.1, \sigma = 51.7$ mmho/m)

Fig. 6. Spectrum and cross-range field pattern of one of the antenna elementsof the antenna shown in Fig. 4.

Table 1 SAF's for Some Simple Geometries

Geometry	SAF
Planar contrast	Γ
Infinite circular cylinder	
axis parallel to antenna	$\Gamma\sqrt{\frac{R_1}{2(R_1+d)}}$
axis perpendicular to antenna	$\Gamma\sqrt{\frac{R_2}{2(R_2+2d)}}$
Contrast with 2 distinct radii of curvature	$\Gamma\sqrt{\frac{R_1}{2(R_1+d)}\frac{R_2}{2(R_2+2d)}}$

dependent and the range dependence is predictable by the geometrical optics result of Table 1. It is also dependent on the conductivity. The conductivity dependence is generated because the reference plane of Fig. 8 is taken at the center of the tunnel. The additional path loss is introduced when the reference E^I propagates twice the distance from the top of the cylinder to the center of the cylinder. If this propagation loss is removed from the results given in Fig. 8 then the geometrical optics SAF of Table 1 is in agreement with Fig. 8 for $f > 10^8$ Hz. The interference pattern is of course the result of reflections from the top and bottom of the tunnel. The SAF have been presented for rectangular as well as for circular tunnels [27] and for circular tunnels containing a wire parallel to the tunnel axis [28].

The quantity V_R'/V_T (see Fig. 7) can be generated by any preferable computation. We have represented this as a pulse attenuation function A. A moment method analysis is suitable for treating the coupling between the dipoles. A Gaussian pulse (Fig. 2) is transmitted and the received pulse is then computed assuming the parameters of the medium are independent of frequency. The pulse attenuation function [29]

$$A = \frac{V_R'(\text{peak})}{V_T(\text{peak})} = A_0 \frac{e^{-2\alpha d}}{2d}. \tag{3}$$

Equation (3) can be rewritten in the form

$$A(\text{dB}) = A_1(\text{dB}) + A_F(\text{dB}) \tag{4}$$

where

$$A_1 = 20 \log_{10} (A_0) \tag{5}$$

and

$$A_f = 20 \log_{10} \frac{e^{-2\alpha(d-1)}}{d} \tag{6}$$

where A_0 has been computed for a depth [29] $d = 1$ m as function of antenna length and electrical parameters of the Earth.

To include the ground interface in the analysis requires a rather tedious Sommerfeld integral be included in the analysis. However, a simple approximation is appropriate [30], [31]. If the fields of the electric line source are simply multiplied by $(1 + \Gamma)$ then a reasonable result is obtained. Figure 9 shows the fields of such a line source under various conditions. The approximate and the exact result are in reasonable agreement for the fields within the Earth. This approach was then used to compute the SAF for a rectangular perturbation within the Earth via an integral equation solution and indeed the approximate and more exact results are again in reasonable agreement. In conclusion, a reasonably accurate result can be generated from

$$V_R = (V_R')\,(\text{SAF})\,(\text{ICF}) \tag{7}$$

where ICF is designated as an interface correction factor.

There are two possible frequency bands of operation for GPR's, defined as the Low-Frequency Window (LFW) and the High-Frequency Window (HFW) by Gabbilard *et al.* [32]. While there is substantial potential for radars operating in LFW, this has not been exploited and is not discussed further in this paper. The frequency band of radars operating in the HFW is defined by [29]

$$d < \frac{8}{\sigma}\sqrt{\frac{\epsilon}{\mu}}. \tag{8}$$

Equation (8) is based on the radiation of an infinitesimal dipole in a lossy homogeneous medium. There can be a dip in these radiated fields as the frequency is increased from zero. Equation (8) is based on restricting that dip to less than 10 dB. Other limitations on the depth of operation of such GPR's include clutter, radio-frequency interference, noise, and available equipment.

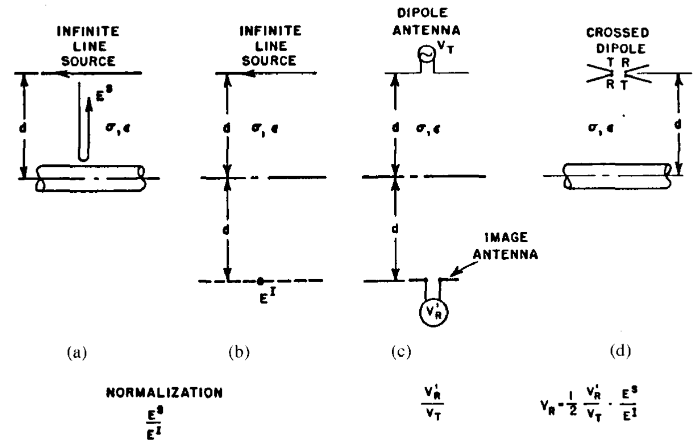

Fig. 7. Introducing the scattering attenuation function of a cylinder into the radar model.

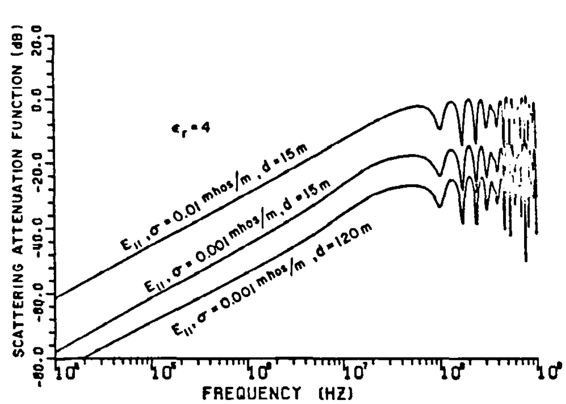

Fig. 8. Comparison of scattering attenuation function for 1-m-radius tunnel for different depths (d) and conductivity (σ) shows that the primary effect of these parameters is to change the amplitude of the curve.

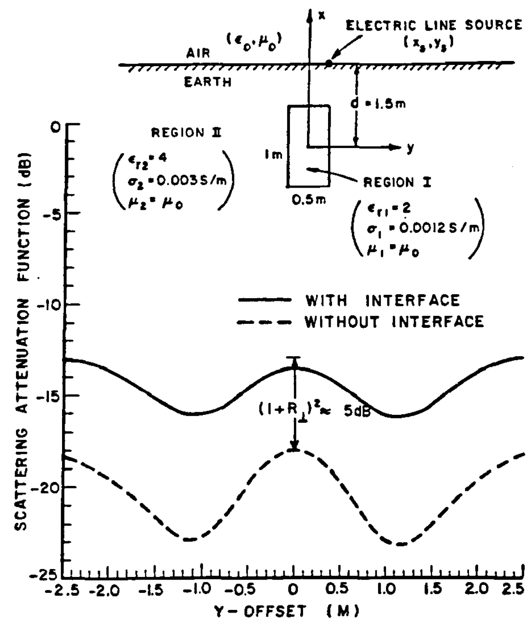

Fig. 9. Comparison of backscattered field patterns of a tunnel geometry, with and without the air–Earth interface. Frequency is 100 MHz.

IV. GPR Field Operations with Emphasis on Environmental Issues

In this section attention is focussed on environmental issues, i.e., on detecting and/or monitoring sites that may be sources of potential pollution. The concept of mapping common to many types of geophysical processing is outlined and several specific types of scatterers of interest to environmental researchers are used to illustrate these concepts.

The present *modus operandi* for GPR produces a two-dimensional cross section (sometimes called a record) of the subsurface that is similar in appearance and interpretation to a seismic cross section. Field operation of a GPR system is very simple and data can be acquired very rapidly. Presently, it is not uncommon to tow the antennas behind an All Terrain Vehicle (ATV) and collect several line-kilometers of data along profile lines spaced a few meters (or fractions of meters) apart. These high data densities ultimately can be exploited to produce three-dimensional images of the subsurface. The mobility and simple field procedures inherent to GPR make it a natural technique for geotechnical applications.

In practice, GPR measurements are made by towing the antennas continuously over the ground. The antennas can be towed by pulling them by hand, or with a vehicle (usually an ATV). A radar wave is transmitted and received each time that the antenna has been moved a fixed distance across the ground surface. Usually, this distance (called the trace spacing) is less than 0.3 m. Every time that the antennas have traveled a distance equal to the trace spacing, the following sequence of events occurs in the GPR system: 1) a wave is transmitted, 2) the receiver is turned on to "wait" to receive reflected signals, and 3) after a certain period of

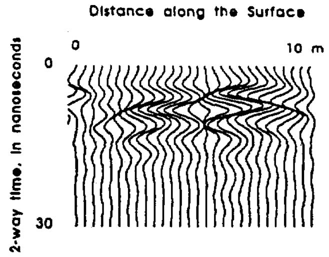

(a)

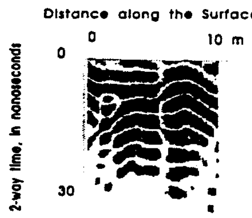

(b)

Fig. 10. Comparison of wiggle trace and gray-scale scan record displays. Anomalies are caused by two buried barrels. (a) Wiggle trace plot. (b) Gray-scale scan plot.

time (usually less than 1 μs) the receiver is turned off. The information that is recorded while the receiver is turned on is called a trace.

A single trace can be used to detect objects (and determine their depth) below a spot on the surface. By towing the antenna over the surface and recording traces at a fixed spacing, a record section of traces (often referred to as a cross section) can be constructed. The horizontal axis of the record section is surface position, and the vertical axis is round-trip travel time of the electromagnetic wave. Two types of recordings of GPR traces are shown in Fig. 10, including: a) a wiggle trace display, where the intensity of the received wave at an instant of time is proportional to the amplitude of the wiggle, and b) a gray-scale display, where the intensity of the received wave at an instant in time is proportional to the intensity of gray scale (i.e., black is high intensity, white is low intensity). The data of Fig. 10 were collected using the Time Domain Monopulse Antenna. The horizontal position of the barrels is determined quite accurately as the position of the minimized waveform or white vertical line for the gray-scale plot.

When the traces are displayed as a cross section, the size, shape, and depth of objects can be determined. The depth to the top of the object is computed by dividing the two-way travel time to the object by twice the velocity of the electromagnetic wave through the ground

$$\text{Depth} = \frac{\text{2-way travel time}}{2 \cdot (\text{velocity of the wave})}. \quad (9)$$

Typical ranges for two-way travel-time range settings are 10 to 500 ns. The velocity of the electromagnetic wave depends primarily upon the relative permittivity (sometimes called the dielectric constant, or dielectric permittivity) of the rock, soil, or other material. The range for relative permittivity values is from 1 (for air) to 81 (for water). In general, the velocity of a radar wave in a material can be calculated from the following relationship:

$$\text{Velocity} = \frac{\text{Velocity of a radar wave through air}}{\sqrt{\text{relative permittivity of the material}}}. \quad (10)$$

The velocity of a radar wave in air is approximately 1 ft/ns (0.305 m/ns). The velocity of a radar wave in water (relative electric permittivity = 81) is equal to 0.0339 m/ns. The relative permittivity of a clean sand, or homogenous granite, is approximately equal to 5, with a velocity of approximately 0.13625 m/ns. In order to interpret the data more accurately, the electrical characteristics of the media are measured at various depths on the day of the experiment. Electrical properties can be measured by inserting a capacitive probe developed by Caldecott *et al.* [33] into a shallow Auger hole. The probe operates at 40 MHz and it is assumed the properties of the media vary slowly with frequency so they can be used to approximate the entire range of consideration. Usually one borehole is used to approximate the test area and measurements are taken at 10-cm depth increments.

A. Applications

GPR has been used primarily to locate engineering and environmental targets in the upper 10 m of the earth. Specific targets for environmental applications include locating buried tanks, drums, landfill debris, geologic structure, water levels, trenches, and contaminated fluids [34]. In civil engineering, GPR is used to locate pipes buried in the ground, imperfections and reinforcing rods within structural concrete, and laminations and voids in roads and bridges. Other common applications of GPR include locating tunnels and other buried voids [35]–[37], and located buried military ordnance [8]–[10], [26]–[29]. In some cases, subsurface targets are resonant scatterers (e.g., metal tanks and drums), or they may be simple one-dimensional reflectors (e.g., stratigraphic layers, or the water table), while in other cases they may be simple nonresonant scatterers (e.g., Earth inhomogeneities). Frequently, the objectives of a GPR survey are to locate all three types of targets from one survey, and the problem for the interpreter is to separate and classify the different targets.

Examples of two-dimensional GPR cross sections over two buried drums and a trench are shown in Fig. 11 for a bistatic antenna instead of the Time Domain Monopulse Antenna (Fig. 3). An example of the response of a monostatic GPR antenna system (500 MHz) over confined diesel fuel and water are shown in Fig. 12. Each of these examples illustrates the hyperbolic anomaly that is characteristic of finite scatterers in the subsurface. The hyperbolic anomaly is caused by moving the transmit and receive antennas over the object, which is analogous to an airborne target moving towards and away from a fixed ground radar. In both cases, Synthetic Aperture Radar (SAR) processing (referred to as migration by geophysicists) may be used to process an improved image of the target. However, complexities associated with multiple scatterers and a heterogenous

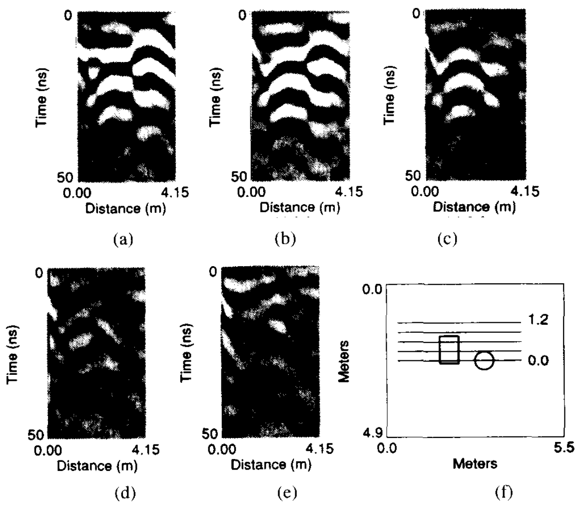

Fig. 11. Parallel polarized data along parallel profile lines at 0.3-m distance increments from the center of the vertical barrel. (a) Center. (b) 0.3 m. (c) 0.6 m. (d) 0.9 m. (e) 1.2 m. (f) Profile lines.

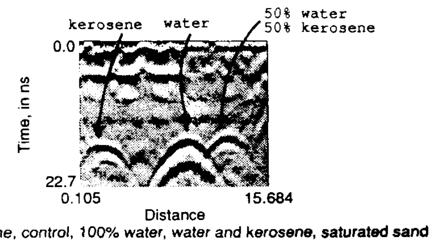

Fig. 12. Test model results of GPR measurements for a 500-MHz antenna over sand saturated with a single fluid.

velocity distribution in the subsurface presents difficulties for SAR/migration processing of GPR data.

Individual horizontal and vertical subsurface features have been identified and interpreted to depths exceeding 10 m using GPR data at a mine in Zortman, MT [38]. The syenite porphyry at the mine is homogenous in its electrical properties except where fracturing, faulting, or sulfide intrusions occur. Fracturing from drilling and blasting operations is generally confined to the region from the surface down to 1–2 m below the surface. The examples in Fig. 13 illustrate GPR anomalies caused by near-surface fractures in the upper 3 m (0–45 ns) for Fig. 13(a) and the upper 1 m for Fig. 13(b) (0 to 16 ns).

GPR anomalies at the mine are generally caused by sulfides, drifts, and vertical features (winzes, manways, and stopes). A typical stope anomaly is shown in Fig. 13(a)., while anomalies caused by mineralogic sulfides and mine drifts are shown in Fig. 13(b). Sulfides generally cause numerous overlapping anomalies, and they often appear as dipping planes when they are associated with veins. The anomaly pattern on the left side of Fig. 13(b) is typical for Zortman sulfide zones. The right side of this zone appears to have an associated fracture that is interpreted as being filled with sulfides causing an anomaly that has characteristics

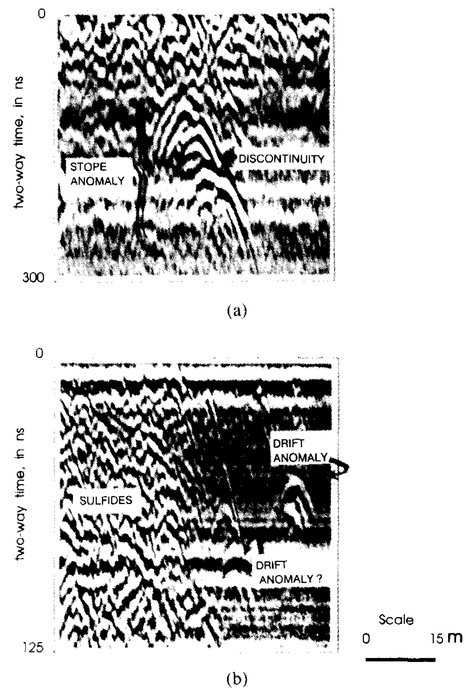

Fig. 13. Examples of GPR anomalies associated with (a) stoping, and (b) sulfides and drifts (from [38]).

similar to a dipping plane as described by Ulriksen [39]. Anomalies caused by drifts (a horizontal passageway) are usually isolated singular anomalies as shown in Fig. 13(b).

Anomalies caused by stopes (a large mined-out region within a drift) are usually complex, containing multiple hyperbolas at different two-way travel times. Open stopes generally yield a very broad, distinct, high-amplitude anomaly that is normally easy to distinguish from a sulfide zone, or a naturally occurring fracture. The lateral discontinuity in the parabola indicated in Fig. 13(a) is common to many vertical features at Zortman. These abrupt lateral changes in the parabolas are thought to be caused by interference between reflections on different boundaries in the vertical structure. The amount of interference is a function of the size and orientation of the features, with the most interference occurring in nearly vertical winzes, or raises that connect the different mining levels (see Fig. 14(e)). Vertical fractures are generally present above the stoped regions. These fracture systems cause additional anomalies on the GPR records, and these anomalies indicate that many of the fractures are associated with stoping extending from the stoped depth to the surface of a level.

Parallel GPR profile lines at the mine were spaced 3.1 m apart, and measurements were made along orthogonal lines when the subsurface workings are oriented in several different azimuthal directions. The GPR records of five parallel lines crossing a major vertical feature are shown in Fig. 14. Since mining operations strip off 6.1 m of rock at each level, the Zortman data set offers the rare opportunity to compare GPR data from different vertical levels. Cor-

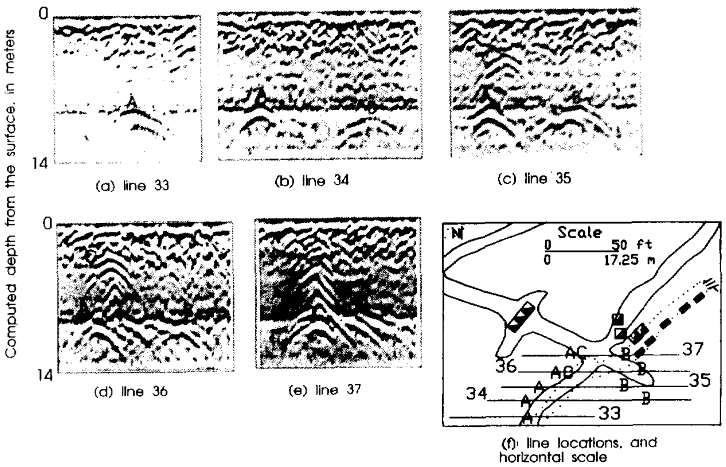

Fig. 14. Sections of GPR lines 33, 34, 35, 36, and 37 across mine workings shown in (f). Horizontal scale of the records is the same as in the index map. Vertical scale is from 0 to 300 ns, or 0 to 14 m, assuming a velocity of 16.4 ns/m (from [39]).

responding adjacent lines for two different vertical levels are shown in Fig. 15. It should be noted that the vertical scales are different on the two data sets. The GPR records in Fig. 15 show a general correlation between the anomalies on the vertically coincident lines. When GPR traverse lines are spaced very closely together, then the closely spaced traces may be treated as a three-dimensional data set, with each trace placed at its x-y surface position, and the vertical axis representing time. An example of three-dimensional display of GPR data for the stoped mining region is shown in Fig. 16.

V. Other Targets

GPR has been used for sensing a wide variety of specific targets. Any object which has electrical parameters different than the surrounding soil and a distinctive shape is a candidate for such efforts.

A. Military Targets

The first GPR uses were in the Vietnam war era. Systems for finding nonmetallic land mines and tunnels were developed, and some of the early patents came out of these efforts. Yet even though systems were developed and tested in the late 1960's and early 1970's for these tasks, this area remains one for continuing development in GPR. This application has significant difficulties due to the propagation losses in the soil, the low contrast between target and soil electrical parameters in some cases, and because of the large variety of clutter echoes from the rough surface and other shallow contrasts such as rocks, tree roots, etc. While it was easy to develop systems which could detect nonmetallic land mines, the discrimination of the mines from clutter under the wide variety of surface and soil conditions has remained very difficult. And the requirement for extremely high detection accuracy (given the danger) as well as very low false alarm rate (given the vast areas to be covered) mean that at least the U.S. Government has not settled on a standard GPR system for this task.

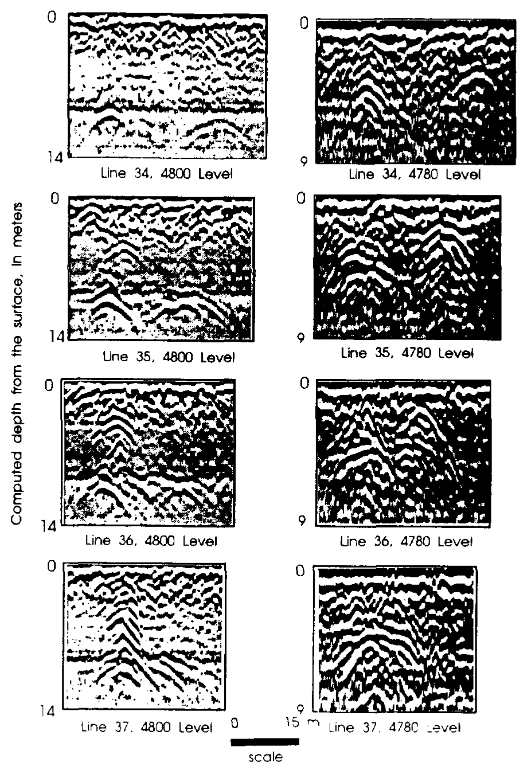

Fig. 15. Comparison of GPR data for coincident lines at two different mining levels (from [39]).

B. Buried Utility Distribution System Targets

Utility location is a continuing use for GPR technology. The need for GPR utility locators was spawned by the use

Fig. 16. 3D display of GPR data, for a line spacing of 3.1 m and a transmit–receive spacing of 0.12 m along the lines.

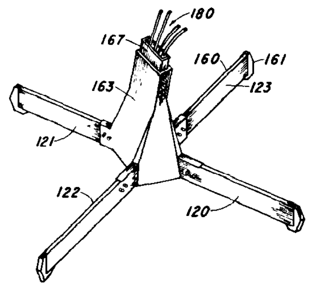

Fig. 17. Crossed-dipole GPR antenna.

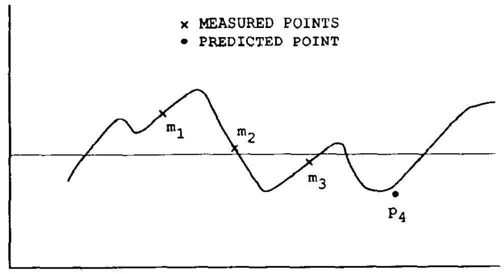

Fig. 18. Illustration of predictor concept.

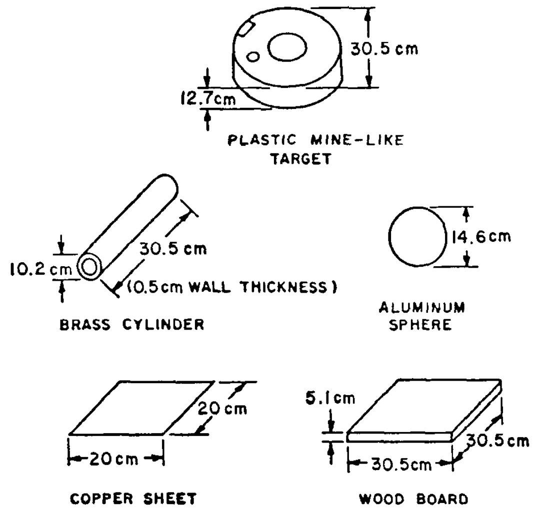

Fig. 19. Physical characteristics of the subsurface targets.

of plastic pipe for natural gas and water distribution. Plastic pipe lasts longer than steel, and does not require a cothodic protection, but it is more vulnerable that steel pipe to sharp digging implements, particularly back-hoe buckets. Also, the plastic pipe cannot be detected or traced using the metal detectors used throughout the utility industry. Conventional practice has been to bury a tracer wire along with the pipes so the metal detectors can still be used. However, there are cases where the tracer has not been buried with the pipe, or has been pulled up, or has deteriorated. Attempts to incorporate a tracer in the plastic pipe walls have affected the strength and longevity of the pipe, and thus have not been successful so far.

The general-purpose profiling systems have been used for this plastic and metal pipe location for many years. Also, a man-portable system was developed starting in the early 1970's. This system, called Terrascan, was covered by several patents, was developed into several prototypes which were tested nationwide, and won an IR 100 Award.

One innovation incorporated in the Terrascan portable pipe locator is a crossed-dipole resistively loaded antenna, shown in Fig. 17. The orthogonal dipoles of this arrangement give excellent transmit–receive isolation, which is important when the antenna-to-target distance is only a few feet, and yet the target echo may be as much as 120 dB down from transmit energy due to interface and propagation losses in the soil, as well as the low target cross section in plastic pipes. The other attractive feature of the crossed-dipole antenna is that horizontal layers such as the water table create no cross-polarized echo, and are thus nearly invisible. However, the antenna does need to be rotated in order to assure that a strong echo from a long thin pipe will be received.

Utility mapping systems have been developed and tested both in the U.S. and in several other countries [40], [41]. In general, the mappers have increased capability compared to the man-portable instrument, but they still require engineering interpretation of the results. One feature which has been clearly identified in utility sensing investigations is the "trench effect" radar return. In many soils, the excavation process at pipe installation alters the soil, and even with the most careful backfilling techniques, the alteration in soil and water drainage properties creates a soil parameter contrast which is almost always evident. This soil parameter contrast creates an extra echo, and can also act as a leaky waveguide to guide more energy down to the pipe when the antenna is directly over the trench. The interpretation and use of this trench echo is controversial in the utility industry. On the one hand, it can provide a strong echo associated with the pipe burial process which comes right up to the surface, and thus is not severely attenuated by the soil. On the other hand, detecting the trench is not identical to detecting the pipe, and sometimes a combination of weather conditions make the trench effect go away. Also, there are several situations where pipe installation techniques (boring in the pipe or laying the pipe and then backfilling a whole layer of soil over the pipe) and soil conditions (like sandy soil) result in no trench effect in conjunction with the pipe.

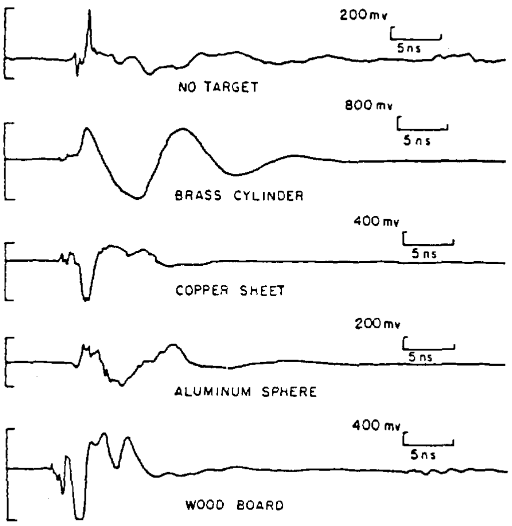

Fig. 20. Processed waveforms from the other subsurface targets.

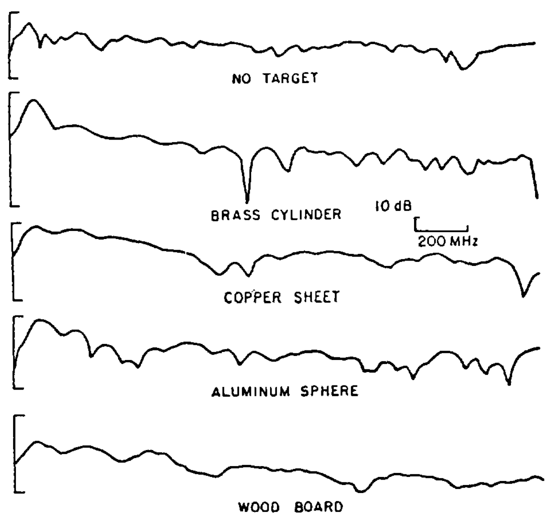

Fig. 21. FFT of the processed waveforms from the other subsurface targets.

C. Highway and Bridge Probing

GPR has been used in highway and bridge sensing with good success. The parameters of concrete, stone, gravel, etc., normally yield good radar signal propagation, even at UHF and microwave frequencies. Results have shown that with processing, GPR can give excellent resolution, and can detect highway features such as voids and moisture pockets, as well as bridge structural flaws [42], [43]. Perhaps the only problem area for GPR in highway remote sensing is created by metal reinforcing mesh. The mesh must be larger than 1/2 wavelength if sensing of layers and flaws beneath the mesh is desired.

D. Burial Detection

Virtually every type of grave creates a contrast in electrical parameters which is detectable with GPR. This includes

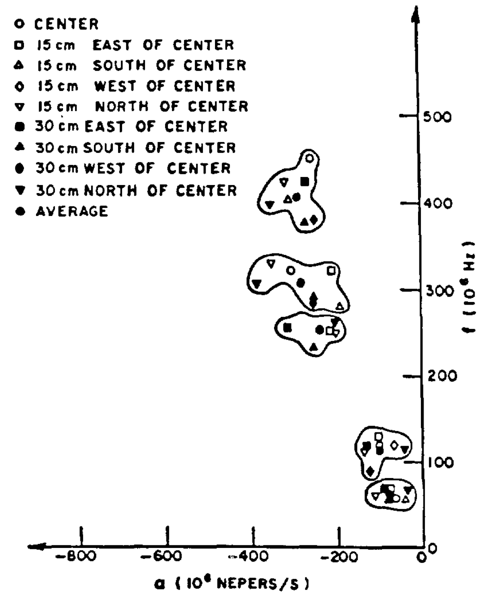

Fig. 22. Location of the extracted resonances of the mine-like target atdifferent antenna locations in icy ground.

the parameters of a body, the parameters of any enclosure of a body, and also the contrast in soil parameters created by the excavation and backfill. Even a small urn with cremation ashes creates a detectable contrast [44]. GPR has been successfully demonstrated for locating a wide variety of burial sites [45], [46].

E. Archeology

There are a wide variety of nonmetallic buried objects and layer contrasts which are of significant interest in archeology, and which can be detected under favorable soil propagation conditions with GPR. However, most archeological sites are complex, so the interpretation of the radar echo information is perhaps the greatest challenge in its use. Successful investigations of a burial mound in Japan [47] and of a hidden chamber in a pyramid in Teneriffe [48] are two examples of GPR use which were reported at the Fourth International Conference on Ground Penetrating Radar in Finland. It is also true that propagation conditions are not always favorable. An earlier effort on the Pyramid of Cheops was not successful in penetrating to detect any chambers. The conductivity of the pyramid rock was much higher than expected.

F. Ice Probing

Ice has electrical parameters which permit GPR probing with significant penetration. Ice also has a complicated morphology with layering and other structure which can provide information on past weather conditions. GPR investigations of ice morphology have been reported recently [49], as well as GPR detection of objects in ice. Notable among detection efforts is the successful detection of buried WW II aircraft in the Greenland ice cap [50].

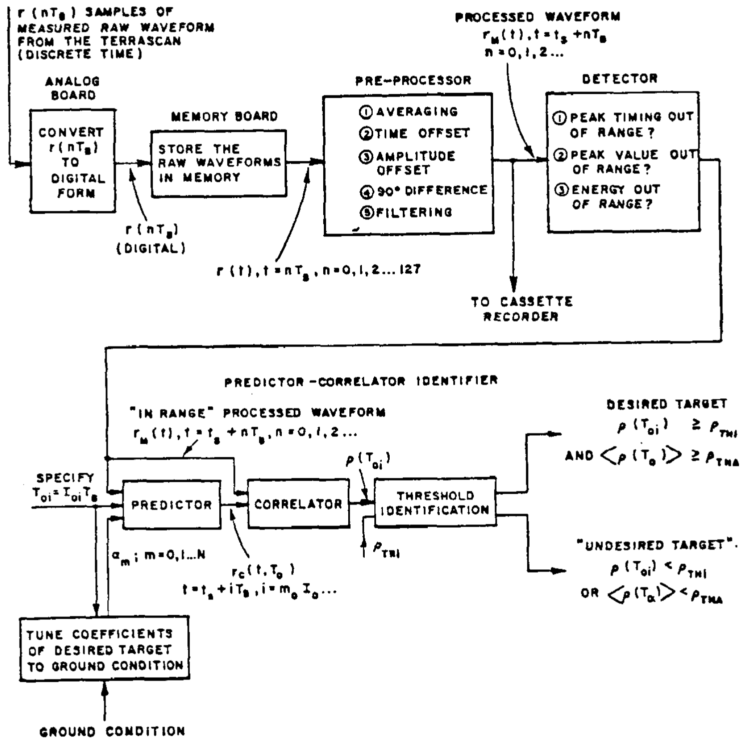

Fig. 23. The identification process implemented in the microcomputer system.

G. Mining Applications

GPR has proven to be a useful tool for remote sensing of the mineral areas being mined in the coal, quarry, and salt mining industries in particular. One important use is to look ahead of the mining process to sense flaws or boundaries which may pose danger or which may indicate the end of good-quality material [51], [52]. Also sensing to determine the stability of mine pillars has been successfully accomplished. As always, GPR success is related to the propagation properties of the medium. Salt has been shown to have about the best possible propagation properties [53]. But coal and minerals such as granite and marble permit GPR use. One challenging area of current research is sensing ahead of tunneling [54].

H. Tunnel Detection

Tunnels in rock or soil create a good electrical parameter contrast with a characteristic path that make them easy to recognize providing soil propagation in the surrounding media give sufficient radar penetration. Tunnels have been detected and identified from the surface at depths of tens of feet in granite [55]. However, a more typical approach for deeper tunnels is to drill vertical boreholes, and perform radar tomography experiments between pairs of boreholes. The radar transmitter and its antenna are positioned at multiple depths in one borehole, and for each transmit depth, the receiver antenna is positioned to receive the radar signals at multiple depths in the adjacent borehole. A tomogram constructed from these records can indicate the presence of the tunnel [56].

VI. Complex Resonances

Complex resonances are one class of GPR response signatures features which may be used for discriminating specific targets from clutter, or for identifying specific target shapes. These features of a target's natural response signature are in general compiled into a library using analysis or laboratory measurements, and then used in a variety of real-time discrimination processes for the real world targets in a high-clutter environment.

A. Characteristic Resonance Concept

To illustrate the concept of CNR's consider a tuning fork. When it is struck it produces an initial transient, which almost instantaneously changes to a simple relatively pure note that may be represented as

$$V = a\cos\omega t e^{-\alpha t} \tag{11}$$

or in polar form

$$V = \mathrm{Re}\left(ae^{j\omega t}e^{-\alpha t}\right). \tag{12}$$

The complex resonance for this case

$$s = -\alpha + j\omega. \tag{13}$$

A more complicated situation arises when more than one note is produced. In this case

$$v = \sum_i a_i e^{S_i t} \tag{14}$$

and

$$S_i = -\alpha_i + j\omega_i. \tag{15}$$

These are the Complex Natural Resonances.

These CNR's have the interesting property of being independent of the excitation. The strength, i.e., the coefficients a_i, are, on the other hand, dependent on the excitation. For the example given, one then must strike the tuning fork at a position where all a_n but the Nth one are zero. Also, the resonances are not evident until after the initial transient. This minimal transient delay time, Δt, was defined by Kennaugh [57].

B. General Features of the Approach

Characteristic resonance discrimination is attractive for GPR applications with the following features:

- The GPR is operated in soils where high frequency propagation is highly attenuated, so that resolution is restricted.
- The GPR is trying to detect a countable number of characteristic "target" types, whose scattering data can be compiled in a library.
- The size of the targets is small enough in wavelengths for the frequencies which can actually propagate through the soil to the target that imaging will not give satisfactory identification.
- The orientation of the buried target is unknown, and a simple discrimination scheme which is nearly independent of orientation is desired.
- The objects to be detected are in the midst of not only soil inhomogeneities, but many false targets of approximately the same echo strength.

Characteristic resonances are also useful for identifying and removing the resonances of some antennas which are used in GPR. Such processing tends to compensate for antenna response in a way which is independent of antenna orientation.

In general, this approach is not useful for:

- targets which have diffuse boundaries, or which have very large extent in one or two dimensions,
- targets which are not resonant, including cases where soil loss damps out the resonances,
- targets which do not have a consistent shape.

C. Specific Applications in GPR

1) Mine Detection and Identification: Early research made use of a GPR consisting of a sampling oscilloscope, a 1-ns pulser, and a cross-dipole antenna. The cross-dipole antenna was perhaps the most important element in this system in that it was practical to observe the reflection from small shallow scatterers with almost no clutter. The task at hand was to then identify the mine using the CNR concept. If

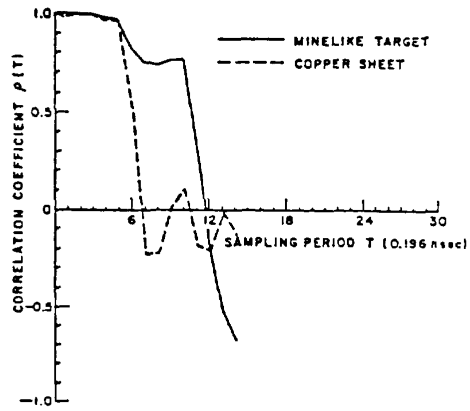

Fig. 24. Typical $\rho(T)$ curves for the identification of the mine-like target in wet ground.

the clutter is sufficiently reduced, the time-domain response can be written as

$$r(t) = \sum_{i=1}^{N} a_i e^{s_i t} \tag{16}$$

where

S_i = complex resonant frequencies (or poles)

a_i = the excitation coefficient (or residues).

Equation (16) may be LaPlace transformed to obtain

$$\mathcal{L}(r(t)) = \sum_{i=1}^{N} \frac{a_i}{(S - S_i)}. \tag{17}$$

Prony enables one to use samples of a waveform to generate an Nth-order difference equation as

$$\sum_{m=0}^{N} \alpha_m r[t + mT] = 0 \tag{18}$$

where T is the sampling interval and the coefficients α_m are determined from the poles S_i and the sampling interval T.

It should be clear that (18) is of the form of a predictor equation. Thus one can use a set of measured points at various sampling times to predict or calculate the response at some other time. For example, (18) can be used to predict the response at $t = NT$ from the measured response from $r(t), r(t+T) \cdots r(t+(N-1)T)$. If this predicted response at NT agrees with the measured response, then this can be used as an identifier. The scheme is illustrated in Fig. 18. This can be automated through the use of a correlation function.

A correlation function can be used to mathematically correlate the measured and computed points in the form

$$P(T) = \frac{\sum_i r_c(t, T) r_m(t)}{\sum_i (r_c^2(t, T) + r_m^2(t))} \tag{19}$$

Table 2 Single-Look Identification Performance for Identification of the Mine-Like Target with the Small-Antenna System

$P_I = 100\%$

Desired Target	Ground Condition	T_c	P_{FA}	P_{FA}	Number of Waveforms		
					Desired	Target	Undesired Target
			$R_{ID} = 30$ cm	$R_{ID} = 45$ cm	$R_{ID} = 30$ cm	$R_{ID} = 45$ cm	
Mine-Like Target	wet	$4T_B$ $5T_B$ $6T_B$ $7T_B$ $8T_B$	1.72%	6.90%	9	13	58

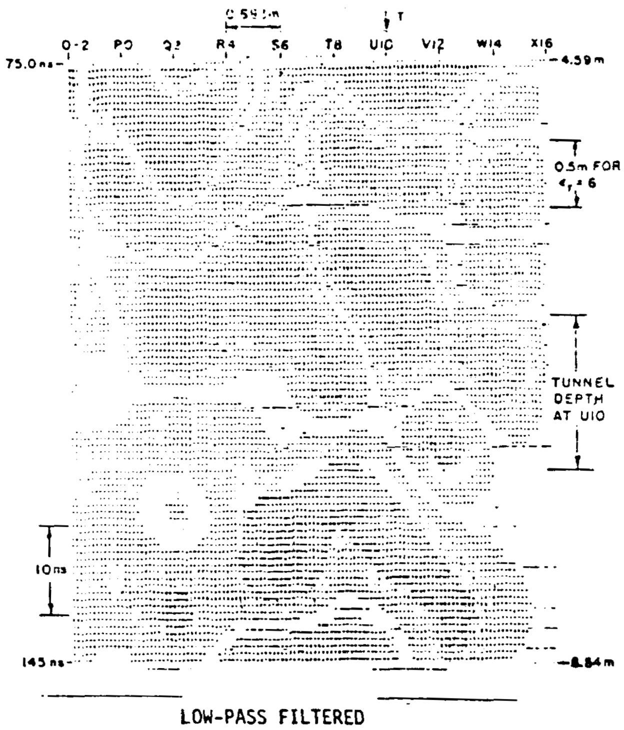

Fig. 25. Mapping of the top traverse over the tunnel as given by Stapp (1978).

where

$$t = iT$$
$$r_c = \text{calculated response}$$
$$r_m = \text{measured response, and}$$
$$T = \text{sampling period.}$$

The sampling period T is a variable. If it is too small, correlation is assured, but identification is not. If it is too large even the desired target will not yield any better correlation.

In the 1970's, a study was made of a series of targets with dimensions of approximately 30 cm as shown in Fig. 19. These were buried in a clay media at a depth of less than 1 ft. A series of GPR measurements were made (time domain). Typical waveform sets and their transforms are shown in Figs. 20 and 21. Clearly, target identification based on these data alone would be impractical with the exception of the brass cylinder where a single strong resonance is apparent. However, the CNR's do provide the necessary identification capability. In the following, one target is to be identified, the others are to be considered to be false targets. A number of other false targets were obtained from measurements over a dirt road bed where the surface roughness and various unknown debris generated echoes.

A typical set of CNR's are given in Fig. 22. These were then inserted in the difference or predictor equation as discussed. The actual processor is shown in Fig. 23. It is observed that the detector block of Fig. 23 was used to discard obvious false targets before the waveform is forwarded to the predictor. It should be noted that this research was pursued before the advent of personal computers. A microprocessor was programmed for this identification and even with this slow technology, identification was achieved in nearly real time. Typical results are indicated in Fig. 24. Table 2 gives target identification of 100% and false alarms less than 10%.

2) Elimination of Undesired CNR's: There is often a strong antenna resonance for most GPR antennas in use today. Most such antennas take the form of heavily loaded dipoles. In spite of the loading, these antennas ring for a period of time. Such reverberations can seriously distort the radar data if the attenuation of the ground is sufficiently strong that the desired signal decays more rapidly as a function of time than the antenna ringing does as a function of time. One such case occurred when measurements were made over a tunnel in the Rocky Mountains. An image created from these GPR data is shown in Fig. 25. Clearly, the results are very distorted. This distortion was introduced by the antenna ringing. The first step consisted of evaluating the CNR's in the raw data. The next step consisted of identifying the CNR associated with the antenna. This antenna resonance was then removed from the raw data.

The complete details are given in [57]. The digital filter to be used to extract this pole pair is obtained by taking the z-transform of the measured waveform $r(t)$. This can be written in the form

$$R(z) = \frac{N(z)}{(1 - z^{-1}z_1)(1 - z^{-1}z_1^*)D(z)} \tag{20}$$

where z_1, z_1^* is the complex pole pair to be removed. The filter process leads to

$$R_p(z) = \left(1 - z^{-1}z_1\right)\left(1 - z^{-1}z_1^*\right)R(z). \tag{21}$$

This can be reduced to

$$R_p(z) = \left[1 - 2\,\mathrm{Re}\,(z_1)z^{-1} + |z_1|^2 z^{-2}\right]R(z). \tag{22}$$

Transformed to the time domain

$$r_p(nT_e) = r(nT_e) - 2\,\mathrm{Re}\,(z_1)r(nT_e - T_e) + |z_1|^2 r(nT_e - 2T_e). \tag{23}$$

One may now carry out the filtering process in the time domain using (23). The points in the filtering process are illustrated in Fig. 26. The point at P_1, T_1 corresponds to $(n-2)T_e$; P_2, T_2 corresponds to $(n-1)T_e$; and P_3, T_3 to nT_e. After completing the steps indicated, the time is increased by T_b and the process is repeated until the pole is filtered out of the entire waveform. Several points need to be made. First, T_e must be selected so that it satisfies the Shannon's sampling theorem, i.e.,

$$T_e \leq \frac{1}{2f_1} \tag{24}$$

where f_1 is frequency of the pole to be removed. Second, the pole pair cannot be removed in the interval $0 < t < 2T_e$.

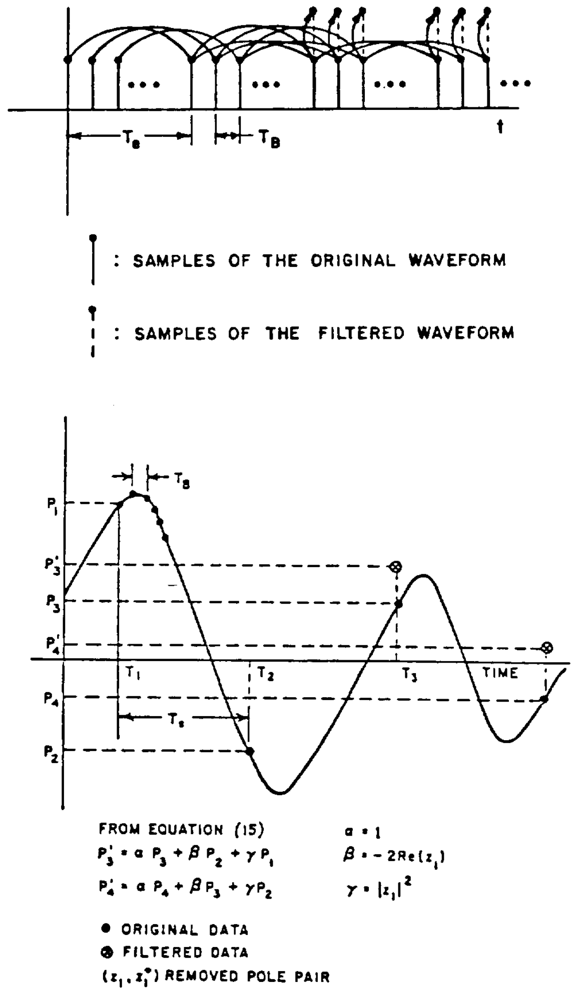

Fig. 26. Demonstration of pole suppression processes.

Volakis considered a waveform with two complex pole pairs given by S_1, $S_1^* = -6 \times 10^6$ Np/s $\pm j2\pi$ 15 $\times 10^6$ rad/s, and S_2, $S_2^* = -6 \times 10^6$ Np/s $\pm j2\pi \times 20 \times 10^6$ rad/s with a residue equal to 2 for both pole pairs. The time-domain expression is given by

$$r(t) = e^{-6\times10^6 t}\cos(30\pi \times 10^6 t) + e^{-6\times10^6 t}\cos(40\pi \times 10^6 t). \tag{25}$$

He extracted the 15-MHz pole from (25). The result is shown in Fig. 27. Clearly, the 20-MHz part of the waveform remains. However, it is distorted both in amplitude and time of arrival. The time is increased by T_e and the amplitude is distorted by the factor

$$AF = 2e^{\sigma_1 T_e}[\cos 2\pi f_2 T_e - \cos 2\pi f_1 T_e]. \tag{26}$$

The last factor in (26) can become small if $f_2 T_e$ and $f_1 T_e$ are nearly equal. Thus the sampling interval T_e is selected to avoid this difficulty. If the final factor in (26) becomes

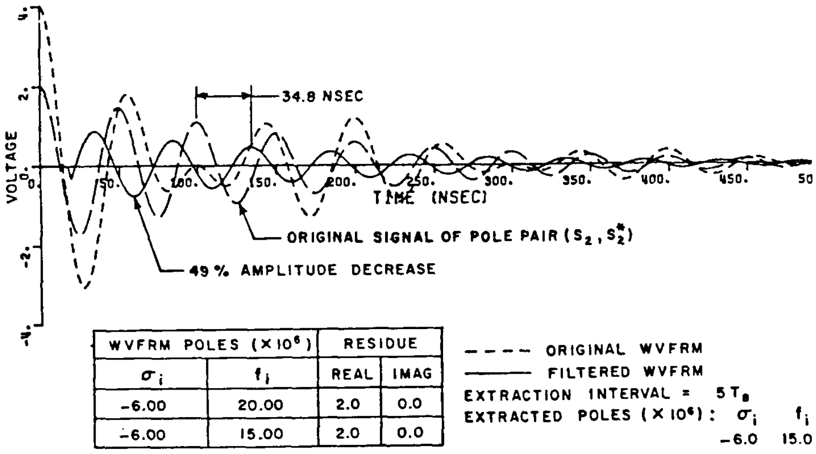

Fig. 27. Example on the amplitude and phase effects due to the pole extraction process.

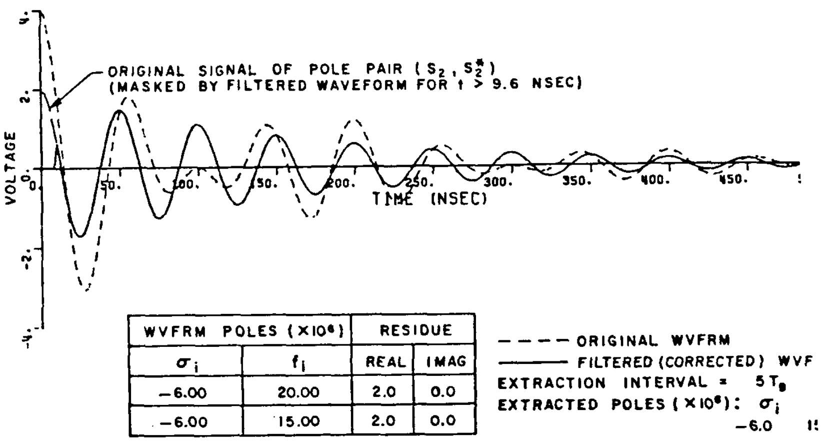

Fig. 28. Application of the correction process to the result of Fig. 27.

negative an additional time increase of

$$\Delta t = \frac{1}{2f_2}$$

is generated.

After applying the corrections as discussed, the waveforms shown in Fig. 28 are generated. Note that the desired pole is not generated until $t > 9.6$ ns, again for reasons discussed earlier. Clearly, after 9.6 ns the desired waveform is reproduced correctly. This process plus an additional backward reconstruction not discussed here was applied to the GPR data used to generate the gray-scale map of Fig. 29. The tunnel is definitely outlined properly. It is noted that there is a precursor (i.e., an image above the tunnel). This is a consequence of the backward reconstruction step not discussed here. However, this reconstructed waveform deviates radically from the measured waveform, since that pole no longer is excited at the earlier time. Thus this precursor is readily identified as such.

D. On-Going Studies

Recent studies of characteristic resonances for identifying buried unexploded ordnance (UXO) are ongoing at The Ohio State University. Discrimination in this application is very important because UXO is normally in the midst of a high concentration of exploded fragments and other clutter. A set of two dozen targets have been measured so far, including inert UXO's, calibration targets, and false targets. Preliminary analysis of the data has been performed. Based on data seen so far, it seems that characteristic resonances are a promising approach to discrimination of buried unexploded ordnance.

VII. Concluding Remarks

There is a great need for the ability to evaluate subsurface parameters without disturbing the ground. One of the most important general areas lies in the environmental area. In the early days of atomic energy development, contaminated materials were buried with little concern of environmental issues. Today no one knows what is buried

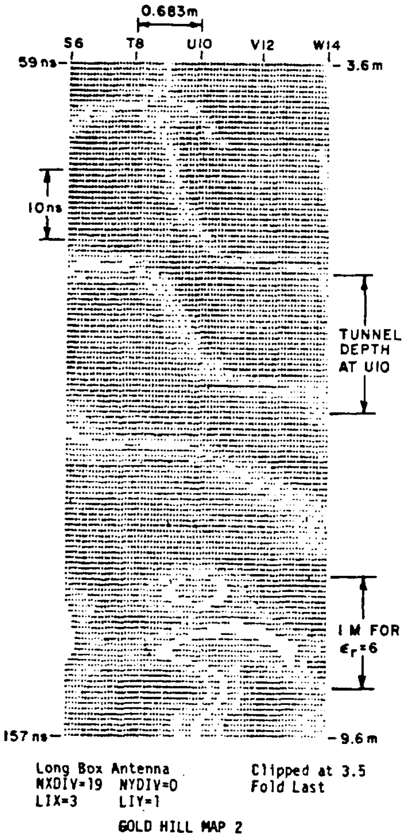

Fig. 29. Mapping of the top traverse over the tunnel.

where. There are also concerns about clearing land used as testing grounds of unexploded ordnance. These are but two examples.

It is essential that any technology used to detect, identify, and locate such buried scatterers be capable of scanning large surface areas rapidly in the presence of clutter etc. Ground Penetrating Radar appears to be a leading candidate for this role.

In this paper, we have attempted to review the state-of-the-art of GPR, suggest several areas where improvement is required, both in terms of the system design and data interpretation. System design would include the stepped frequency systems instead of the base band pulsers currently in use and continuing improvements in antenna design and matching.

Several examples have been included that are of direct interest to environmentalists including fluid saturated soils and barrels. These and several other examples were used to illustrate various mapping concepts as a means of identifying and/or locating scattering mechanisms. A brief but certainly not an all-inclusive overview of other GPR applications is given. Finally, the Complex Natural Resonance concepts are used to both improve the quality of mapping and as a means of scatterer discrimination. There remains much to be achieved in this area particularly in terms of time–frequency distribution.

REFERENCES

[1] L. Peters, Jr., and M. Barnes, "Ground penetrating radar antenna systems operating in the high frequency window," Tech. Rep. 721506-2, The Ohio State University Electro-Science Laboratory, prepared for Environmental Protection Agency under Contract CR-814928-01-0, Oct. 1989.

[2] L. Peters, Jr., and J. D. Young, "Applications of subsurface transient radar," in *Time Domain Measurements in Electromagnetics*, E. K. Miller, Ed. New York: Van Nostrand Reinhold, 1986, pp. 297–351.

[3] J. D. Young, R. Caldecott, and L. Peters, Jr., "Underground radar research at Ohio State University," *IEEE Antennas Propagat. Soc. Newsletter*, pp. 5–8, Aug. 1979.

[4] Workshop on Geophysics for Noninvasive Waste Site Characterization sponsored by Department of Energy, Dallas, TX, Aug. 29–30, 1991.

[5] Workshop on Mine Detection sponsored by Army Research Office and Belvoir Research and Development Center, Durham, NC, June 22–23, 1992.

[6] Range Cleanup Workshop sponsored by U.S. Army Proving Ground, Monterey, CA, Mar. 22–23, 1993.

[7] R. M. Lerner, "Ground radar system," U.S. Patent 3 831 173, 1974.

[8] L. C. Chan, D. L. Moffatt, and L. Peters, Jr., "A characterization of sub-surface radar targets," *Proc. IEEE*, vol. 67, no. 7, pp. 991–1001, July 1979.

[9] ——, "Estimation of complex natural resonances from a class of sub-surface targets," in *Acoustic Electromagnetic and Elastic Wave Scattering-Focus on T-matrix Approach*. New York: Pergamon Press, 1979, pp. 453–463.

[10] ——, "Improved performance of a subsurface radar target identification system through antenna design," *IEEE Trans. Antennas Propagat.*, vol. AP-29, no. 2, pp. 307–311, Mar. 1981.

[11] R. Morey, 1974, U.S. Patent 3 806 795.

[12] J. D. Young and R. Caldecott, "Underground pipe detector," U.S. Patent 3 967 282, 1976.

[13] ——, "Underground pipe detector," U.S. Patent 4 062 010, 1977.

[14] A. C. Eberle and J. D. Young, "Development and field testing of a new locator for buried plastic and metallic utility lines," in *Transportation Research Record 631*, National Academy of Science, 1977.

[15] P. Hänninen and S. Autio, Eds., "Geological survey of Finland," Special Paper 16, presented at the 4th Int. Conf. on Ground Penetrating Radar, June 8–13, 1992.

[16] Third International Conference on Ground Penetrating Radar, Lakewood, CO, May 14–18, 1990.

[17] Advanced Ground Penetrating Radar: Technologies and Applications, Second Government Workshop on GPR, The Ohio State University, Oct. 26–28, 1993.

[18] "Assessment of Ultra-Wideband (UWB) Technology," prepared for OSD/DARPA by Battelle under Contract DAAH-01-88-C-0131, July 1990.

[19] G. Burrell and L. Peteres, Jr., "A Computational model for ground penetrating radar operating in the high frequency window" to be published in a Special Issue of the *J. Appl. Geophys.*.

[20] M. A. Poirier, "Advanced ground penetrating radar," to be published in a Special Issue of the *J. Appl. Geophys.*.

[21] M. Barnes, M. Poirier, and L. Peteres, Jr., "Novel GPR antennas," to be published in a Special Issue of the *J. Appl. Geophys.*.

[22] J. L. Volakis and L. Peteres, Jr., "Improved identification of underground targets using video pulse radars by elimination of undesired natural resonances," *IEEE Trans. Antennas Propagat.*, vol. AP-31, no. 2, pp. 334–340, Mar. 1983.

[23] A. Lai, A. L. Sinopoli, and W. D. Burnside, "A novel antenna for ultra-wideband applications," *IEEE Trans. Antennas Propagat.*, vol. 40, no. 7, pp. 755–760, July 1992.

[24] E. M. Nassar, "Aperture distributions generated by transmission line feed structures," M.Sc. Thesis, The Ohio State Univ., 1993.

[25] W. D. Burnside and T. Barnum, "Fast settling 2 to 18 GHz synthesizer," Tech. Rep. 721929-25, prepared for NASA, Langley Research Center under Grant NSG-1613, Apr. 1990.

[26] G. Burrell and L. Peteres, Jr., "A scattering model for GPR operating in the HFW," to be published in a Special Issue of the *J. Appl. Geophys.*.

[27] L. Peters, Jr., and J. H. Richmond, "Scattering from cylindrical inhomogeneities in a lossy medium," *Radio Sci.*, vol. 17, no. 5, pp. 973–987, Sept.–Oct. 1982.
[28] L. Peteres, Jr., G. A. Burrell, and H. B. Tran, "A scattering model for detection of tunnels using video pulse systems," Tech. Rep. 4460-3, The Ohio State Univ. ElectroScience Lab., prepared for U.S. Army Mobility Equipment Research and Development Command under Contract DAAG53-76-C-0179, Feb. 1977.
[29] G. A. Burrell, L. Peters, Jr., and A. J. Terzouli Jr., "The propagation of electromagnetic video pulses with application to subsurface radar for tunnel application," Tech. Rep. 4460-2, The Ohio State Univ. ElectroScience Lab., prepared for U.S. Army Mobility Equipment Research and Development Command under Contract DAAG53-76-C-0179, Dec. 1976.
[30] J. S. Izadian, L. Peters, Jr., and J. H. Richmond, "Computation of scattering from penetrable cylinder with improved numerical efficiency," *IEEE Trans. Geosci. Remote Sensing*, vol. GE-22, no. 1, pp. 52–61, Jan. 1984.
[31] C. W. Davis, III, L. Peters, Jr., and J. D. Young, "A moment method model for a linear antenna placed at a conducting interface," to be published in a Special Issue of the *J. Appl. Geophys.*.
[32] R. Gabbilard, P. Degauge, and J. R. Wait, "Subsurface Electromagnetic telecommunication—A review," *IEEE Trans. Commun. Technol.*, vol. COM-19, pp. 1217–1228.
[33] R. Caldecott, M. A. Poirier, and D. Svoboda, "A radio frequency probe to measure soil electrical parameters," to be published in the *J. Appl. Geophys.*.
[34] J. J. Daniels and R. L. Roberts, "Ground penetrating radar for geotechnical applications," *Geophysical Characterization of Sites, American Society of Civil Engineers*, ISSMFE TC #10 Publication on Geophysics, special volume XIII ICSMFE, 1994, New Delhi, India.
[35] J. J. Daniels, "Locating caves, tunnels, and mines: the leading edge of exploration," *Soc. Expl. Geophys.*, Jan–Feb. 1988.
[36] J. J. Daniels, "Fundamentals of ground penetrating radar," in *Proc. Symp. on the Application of Geophysics to Engineering and Environmental Problems* (Golden, CO, Mar. 13–16, 1989), p. 80.
[37] J. Daniels, R. Roberts, and M. Vendl, "Site studies of ground penetrating radar for monitoring petroleum product contaminants," in *Trans. Symp. on the Application of Geophysics to Engineering and Environmental Problems*, Apr. 26–29, 1992.
[38] J. J. Daniels, R. Roberts, B. Schilling, and R. Erickson, "GPR measurements for locating underground mine workings at an active open-pit mine," in *Trans. 4th Int. Conf. on Ground Penetrating Radar* (Rovaniemi, Finland, June 8–13, 1992).
[39] P. Ulriksen, "Application of impulse radar to civil engineering," Ph.D. Thesis, Lund Univ. of Technol., Lund, Sweden, 1982.
[40] R. Caldecott, J. D. Young, J. P. Hall, and A. J. Terzuoli, "An underground obstacle detection and mapping system," EPRI Rep. EL-3984, May 1985.
[41] T. Suzuki and I. Arai, "Advance on underground radars," *IEICE Trans.*, vol. E74, no. 2, Feb. 1991.
[42] N. S. Parry and J. L. Davis, "GPR systems for roads and bridges," in *Proc. 4th Int. Conf. on Ground Penetrating Radar* (Rovaniemi, Finland, June 1992).
[43] K. R. Masar and T. Skullion, "Automated pavement subsurface profiling using radar: case studies of four SHRP sites," Transportation Res. Board Rep. 910796, Jan. 1991.
[44] R. R. Unterberger, "Ground penetrating radar finds disturbed Earth over burials," in *Proc. 4th Int. Conf. on Ground Penetrating Radar* (Rovaniemi, Finland, June 1992).
[45] B. W. Bevan, "The search for graves," *Geophys.*, vol. 56, no. 9, pp. 1310–1319.
[46] J. S. Mellett, "Location of human remains with ground penetrating radar," in *Proc. 4th Intl. Conf. on Ground Penetrating Radar* (Rovaniemi, Finland, June 1992).
[47] D. Goodman and Y. Nishimura, "2-D synthetic radargrams for archeological investigation," in *Proc. 4th Int. Conf. on Ground Penetrating Radar* (Rovaniemi, Finland, June 1992).
[48] F.-N. Kong, J. Kristiansen, and T. L. By, "A radar investigation of pyramids," in *Proc. 4th Int. Conf. on Ground Penetrating Radar* (Rovaniemi, Finland, June 1992).
[49] K. C. Jezek, S. A. Arcone, S. Daly, and R. H. Wills, "Impulse radar studies of interface roughness," *Ground Penetrating Radar*, Geo. Survey of Canada Paper 90-4, pp. 107–115.
[50] A. Kovacs, "Electromagnetic sounding in a successful search for buried WWII aircraft on the Greenland ice cap," in *Proc. 3rd Int. Conf. on Ground Penetrating Radar* (Lakewood, CO, May 1990).
[51] M. Piccolo, "GPR application for the definition of unconformities in a Carrara marble quarry," in *Proc. 4th Int. Conf. on Ground Penetrating Radar* (Rovaniemi, Finland, June 1992).
[52] R. Benson and L. Yuhr, "Assessment of bauxite reserves using ground penetrating radar," in *Proc. 4th Int. Conf. on Ground Penetrating Radar* (Rovaniemi, Finland, June 1992).
[53] R. R. Unterberger, "Some GPR results in salt and potash mines," in *Proc. 3rd Int. Conf. on Ground Penetrating Radar* (Lakewood, CO, May 1990).
[54] A. F. Kathage, "A challenge: GPR in advance of horizontal drilling," in *Proc. 4th Int. Conf. on Ground Penetrating Radar* (Rovaniemi, Finland, June 1992).
[55] R. Caldecott, L. Peters, *et al.*, "A re-examination of the potential of video pulse radars for the detection of tunnels in hard rock media," presented at the Symp. on Tunnel Detection, Colorado School of Mines, Golden, CO, July 1981.
[56] R. Kemerait, "What improvement in tunnel detection and identification can be achieved by utilizing tomographic techniques," in *Proc. 2nd Government Workshop on GPR* (Columbus, OH, 1993).
[57] E. M. Kennaugh, "The K-pulse concept," *IEEE Trans. Antennas Propagat.*, vol. AP-29, pp. 327–331, Mar. 1981.
[58] J. L. Volakis and L. Peteres, Jr., "Improved identification of underground targets using video pulse radars by elimination of undesired natural resonances," *IEEE Trans. Antennas Propagat.*, vol. AP-31, no. 2, pp. 334–340, Mar. 1983.

Additional References

- A. P. Annan, W. M. Waller, D. W. Strangeway, J. R. Rossiter, J. D. Redman, and R. D. Watts, "The electromagnetic response of a low-loss, 2-layer, dielectric Earth for horizontal electric dipole excitation," *Geophys.*, vol. 40, p. 285–298, 1975.
- A. P. Annan and J. L. Davis, "Radar range analysis for geological materials, report of activities," *Geological Survey of Canada*, paper 77-1B, pp. 117–124, 1977.
- A. P. Annan, J. L. Davis, and D. Gendswill, "Radar sounding in potash mines, Saskatchewan, Canada," *Geophys.*, vol. 53, no. 12, pp. 1556–64, Dec. 1988.
- V. A. Andrianov, "Subsurface radar of the layered-inhomogeneous soil of a planet," *J. Commun. Technol. Electron.*, vol. 38, no. 5, pp. 16–28, 1993.
- I. Arai and T. Suzuki, "Experimental results on subsurface radar with improved resolution," *J. Electromagn. Waves Appl.*, vol. 7, no. 11, pp. 1479–95, 1993.
- W. Baoyi, X. Runming, D. Yangjian, and Y. Huiqing, "Nanosecond electromagnetic pulse for detecting underground pipes and holes," *Acta Electron. Sin.*, vol. 20, no. 12, pp. 36–41, Dec. 1992.
- V. I. Barantsov, "Characteristics of short-pulse radar probing of deeply buried objects," *Sov. J. Commun. Technol. Electron.*, vol. 34, no. 3, pp. 160–163.
- C. L. Britt, "Solution of electromagnetic scattering problems using time domain techniques," *IEEE Trans. Antennas Propagat.*, vol. 37, no. 9, pp. 1181–1192, 1989.
- G. A. Burrell and L. Peteres Jr., "Pulse propagation in lossy media using the low-frequency window for video pulse radar application," *Proc. IEEE*, vol. 67, no. 7, 1979.
- G. A. Burrell, J. H. Richmond, L. Peters, Jr., and H. B. Tran, "A scattering model for detection of tunnels using video pulse radar systems," in *Acoustic, Electromagnetic and Elastic Wave Scattering—Focus on T-Matrix Approach.* New York, Pergamon, 1979, pp. 667–683.
- J. L. Davis, "Relative permittivity measurements of a sand and clay soil *in situ*," *Geological Survey of Canada*, paper 75-1C, pp. 361–363, 1975.
- J. L. Davis, G. C. Topp, and A. P. Omran, "Measuring soil water content *in situ* using time domain reflectometry techniques," *Geological Survey of Canada*, paper 77-1B, pp. 33–36, 1977.
- J. L. Davis and A. P. Annan, "Ground-penetrating radar for high-resolution mapping of soil and rock stratigraphy," *Geophys. Prospect.*, vol. 37, no. 5, pp. 531–51, July 1989.
- P. Degauge and J.-P. Thery, "Electromagnetic subsurface radar using the transient field radiated by a wire antenna," *IEEE*

Trans. Geosci. Remote Sensing, vol. GE-24, no. 6, pp. 805–12, Nov. 1986.
- K. Deguchi, T. Okada, and I. Morishita, "Analysis of underground radar image using generalized hough transformation technique," *Trans. Soc. Instrum. Control Eng.*, vol. 25, no. 7, pp. 800–807, July 1989.
- K. A. Dines and R. J. Lytle, "Computerized geophysical tomography," *Proc. IEEE*, vol. 67, no. 7, 1979.
- B. A. Falls, "Apparatus for measuring the electromagnetic impedance of soils," U.S. Patent 4013950, 1977.
- E. Fisher, G. A. McMechan, and A. P. Annan, "Acquisition and processing of wide-aperture ground-penetrating radar data," *Geophys.*, vol. 57, no. 3, pp. 495–504, Mar. 1992.
- E. Fisher, G. A. McMechan, A. P. Annan, and S. W. Cosway, "Examples of reverse-time migration of single-channel, ground-penetrating radar profiles," *Geophys.*, vol. 57, no. 4, pp. 577–86, Apr. 1992.
- Y. He, "A study of inverse scattering problems of a underground metal cylinder," *Rec. Electr. Commun. Eng.* (Conversazione Tokuhu Univ.), vol. 57, no. 4, June 1989.
- A. Helaly, L. Shafai, and A. Sebak, "Low-frequency response of a buried object in a lossy ground," *Conv. Phys.*, vol. 68, no. 1, pp. 111–120, Jan. 1990.
- P. Hoekstra and A. Delaney, "Dielectric properties of soils at UHF and microwave frequencies," *J. Geophys. Res.*, vol. 79, no. 11, pp. 1699–1708, 1974.
- R. T. Houck, "Measuring the electrical properties of coal using ground-penetrating radar," *IEEE Trans. Geosci. Remote Sensing*, vol. GE-23, no. 6, pp. 851–854, Nov. 1985.
- K. Ingulsa and A. P. Freundhorfer, "A method of surface clutter cancellation for an underground CW radar," *IEEE Trans. Electromagn. Compat.*, vol. 31, no. 3, pp. 330–332, 1989.
- H. M. Jol and D. G. Smith, "Ground penetrating radar of northern lacustrine deltas," *Can. J. Earth Sci.*, vol. 28, no. 12, pp. 1939–1947, Dec. 1991.
- M. Kora, Y. Seki, H. Ishikawa, Y. Watanabe, A. Kaneda, K. Fujii, and T. Saikyo, "Subsurface radar," *JRC Rev.*, no. 25, pp. 31–7, 1987.
- X. Lei and Z. Lihe, "3-D object image reconstruction from returns of subsurface radars," *Acta Electron. Sin.*, vol. 19, no. 3, pp. 121–123, May 1991.
- O. Maeshima, T. Uno, Y. He, and S. Adachi, "FDTD analysis of transient cylindrical electromagnetic wave scattered by objects buried in a two-dimensional inhomogeneous medium," *Trans. Inst. Electron. Inf. Commun. Eng.*, vol. J76B-II, no. 2, pp. 138–44, Feb. 1993.
- ——, "FDTD analysis of two-dimensional cavity-backed antenna for subsurface radar," *IEICE Trans. Electron*, vol. E76-C, no. 10, pp. 1468–1473, Oct. 1993.
- Y. Michiguchi, K. Hiramoto, M. Nishi, F. Takahashi, T. Ohtaka, and M. Okada, "Development of signal processing methods for imaging buried pipes," *IEEE Trans. Geosci. Remote Sensing*, vol. GE-25, no. 1, pp. 11–15, Jan. 1987.
- Y. Michiguchi, K. Hiramoto, M. Nishi, T. Ohtaka and M. Okada, "Advanced subsurface radar system for imaging buried pipes," *IEEE Trans. Geosci. Remote Sensing*, vol. 26, no. 6, pp. 733–740, Nov. 1988.
- D. L. Moffatt and R. J. Puskar, "A subsurface electromagnetic pulse radar," *Geophys.*, vol. 41, pp. 506–518, 1976.
- Y. Nagashima and J. Mosuda, "Underground radar apparatus using pattern recognition in frequency domain," *NTT R&D*, vol. 38, no. 6, pp. 667–676.
- I. J. Paoloni, "Imaging of buried objects using an impulse radar model," *J. Electr. Electron. Eng. Aust.*, vol. 13, no. 1, pp. 32–40, Mar. 1993.
- I. C. Peden, R. Kipp, and J. Allestad, "A scale-model study of down-hole VHF dipole arrays with application to subsurface exploration," *IEEE Trans. Geosci. Remote Sensing*, vol. 30, no. 5, pp. 885–891, Sept. 1992.
- P. V. Riad and J. L. Nicol, "Input admittance of a horizontal antenna over a 2-layered lossy half-space," *Radio Sci.*, vol. 25, pp. 27–35, Jan.–Feb. 1990.
- J. Schneider and I. C. Peden, "Detection of tunnels in low loss media illuminated by a transient pulse," *IEEE Trans. Geosci. Remote Sensing*, vol. 31, no. 2, pp. 503–506, Mar. 1993.
- W. R. Scott, Jr., and G. S. Smith, "Measured electrical constitutive parameters of soil as functions of frequency and moisture content," *IEEE Trans. Geosci. Remote Sensing*, vol. 30, no. 3, pp. 621–623, May 1992.
- A. F. Siggins, "Ground penetrating radar in geotechnical applications," *Explor. Geophys.*, vol. 21, no. 3–4, pp. 175–186, Sept.–Dec. 1990.
- M. Skolnik, D. Hemenway, and J. P. Hansen, "Radar detection of gas seepage associated with oil and gas deposits," *IEEE Trans. Geosci. Remote Sensing*, vol. 30, no. 3, pp. 630–633, May 1992.
- D. G. Smith and H. M. Jol, "Ground-penetrating radar investigation of a Lake Bonneville Delta, Provo Level, Brigham City, Utah," *Geology*, vol. 20, no. 12, pp. 1083–1086, Dec. 1992.
- G. S. Smith and W. R. Scott, Jr., "A scale model for studying ground penetrating radars," *IEEE Trans. Geosci. Remote Sensing*, vol. 27, no. 4, pp. 358–363, July 1989.
- T. Suzuki, "A study of EM fields scattered by underground objects," *Rec. Electr. Commun. Eng.* (Conversazione Tokuhu Univ.), vol. 57, no. 4, June 1989.
- T. Suzuki and I. Arai, "Advance on underground radars," *IEICE Trans.*, vol. E74, no. 2, pp. 189–194, Feb. 1991.
- K. Taketomi and Y. Miyazaki, "Underground cavity detection using statistical variance of subsurface radar signal," *Trans. Soc. Instrum. Control Eng.*, vol. 29, no. 6, pp. 653–658, June 1993.
- T. Usami, H. Ohnishi, S. Odagiri, Y. Uekubo, and A. Jitsumori, "Detection of the underground pipes by synthetic aperture techniques," *Trans. Inst. Electron. Commun. Eng. Japan. E. Engl.*, vol. E69, no. 4, pp. 491–493, Apr. 1986.
- C. J. Vaughan, "Ground penetrating radar survey used in archaeological investigations," *Geophys.*, pp. 595–604, Mar. 1986.
- A. R. Von Hippel, Ed., *Dielectric Materials and Applications*. Cambridge, MA: M.I.T. Press, 1961, p. 438.
- J. R. Wait, "Mutual electromagnetic coupling of loops over a homogeneous ground," *Geophys.*, vol. 20, no. 3, pp. 630–637, 1955.
- J. R. Wait and K. A. Nabulsi, "Preforming an electromagnetic pulse in lossy medium," *Electron. Lett.*, vol. 28, no. 6, pp. 542–543, Mar. 12, 1992.
- B. G. Warner, D. C. Nobes, and B. D. Theimer, "An application of ground penetrating radar to peat stratigraphy of Ellice Swamp, Southwestern Ontario," *Can. J. Earth Sci.*, vol. 27, no. 7, pp. 932–938, July 1990.
- P. Waters, D. Greenbaum, P. L. Smart, and H. Osmaston, "Applications of remote sensing to groundwater hydrology," *Remote Sens. Rev.*, vol. 4, no. 2, pp. 223–64, 1990.
- W. A. Wensink, G. Greeuw, J. Hofman, and J. K. Van Deen, "Measured underwater near-field E-patterns of a pulsed, horizontal dipole antenna in air; Comparison with the theory of the continuous wave infinitesimal electric dipole," *Geophys. Prospect.*, vol. 38, no. 7, pp. 805–830, Oct. 1990.
- W. A. Wensink, J. Hofman, and J. K. Van Deen, "Measured reflections strengths of underwater pipes irradiated by a pulsed horizontal dipole in air: Comparison with continuous plane-wave scattering theory," *Geophys. Prospect.*, vol. 39, pp. 543–566, 1991.

Leon Peters, Jr. (Life Fellow, IEEE) was born in Columbus, OH. He received the B.E.E., M.Sc., and Ph.D. degrees from The Ohio State University, Columbus, in 1950, 1954, and 1959, respectively.

In 1950 he became a Research Associate in the ElectroScience Laboratory (formerly Antenna Laboratory), Department of Electrical Engineering, The Ohio State University, where he is now the Director. In 1960 he joined the teaching staff at The Ohio State University, where he is now a Professor Emeritus in the Department of Electrical Engineering. He has served as Technical Area Director for electromagnetic and remote sensing and as the Associate Department Chairman for Research. His primary interests are in the fields of antennas, microwaves, and properties of radar targets.

Dr. Peters is a member of Sigma Xi and Commision B of the International Union of Radio Science.

Jeffrey J. Daniels received the Ph.D. degree in geophysical engineering from the Colorado School of Mines in 1974.

He is an Associate Professor in the Department of Geological Sciences at The Ohio State University (OSU), Columbus. He worked for the U.S. Geological Survey from 1974 until joining the faculty at OSU in 1985. His research activities at OSU have been primarily concerned with developing new processing and interpretation approaches for GPR data, with primary applications to shallow engineering and environmental applications.

Dr. Daniels is a member of AGU, SEG, SPWLA, and is Past President of the newly formed Environmental and Engineering Geophysical Society (EEGS).

Jonathan D. Young (Member, IEEE) received the B.E.E. (summa cum laude), M.Sc., and Ph.D. degrees from The Ohio State University, Columbus, in 1964, 1965, and 1971, respectively.

He has been on staff at The Ohio State University ElectroScience Laboratory since 1971. He has been engaged in research on radar target scattering signatures and imaging, ultra-wideband radar antennas, measurements, and scattering analysis, and Ground Penetrating Radar studies during that time. Since 1983, he has also been serving as the Associate Director of the ElectroScience Laboratory. During the years 1991–1994, he has served on the Ohio State University Research Committee. His recent studies on radar target scattering diagnostics have concentrated on measurements and analysis of scattering phenomenology at frequencies below 2 GHz, where foliage penetrating radars operate. He has been a pioneer in Ground Penetrating Radar system research and development. He holds 4 patents on the Terrascan, a radar buried utility locator system for detecting plastic as well as metal pipes. This system won an IR100 Award from *Industrial Research Magazine* in 1978. His recent GPR studies concentrated on systems which can combine target identification with detection for buried targets. Some of his most recent research involves the application of radar sensing to Automated Highway system needs.

Dr. Young is a member of Tau Beta Pi, Eta Kappa Nu, and Sigma Xi. He held offices in the local IEEE AP-S Chapter during 1984–1986, when the chapter won two outstanding chapter awards.